CHAPTER 11 ■ MEDIASTINUM AND HILA

JEFFREY S. KLEIN

This chapter will review the radiologic approach to mediastinal masses, diffuse mediastinal disease, and hilar abnormalities.

MEDIASTINAL MASSES

Localized mediastinal abnormalities are common diagnostic challenges for the radiologist. Patients with mediastinal masses tend to present in one of three ways: (1) with symptoms related to local mass effect or invasion of adjacent mediastinal structures (e.g., stridor in a patient with thyroid goiter); (2) as the result of a search for mediastinal abnormality in a patient with a predisposing condition (e.g., a patient with myasthenia gravis and concern for thymoma); or (3) as an incidental finding on chest radiography or CT. Occasionally, a mediastinal mass is discovered in the course of an evaluation for known malignancy (e.g., a patient with non-Hodgkin lymphoma [NHL]). Contrast-enhanced multidetector row CT (MDCT) is the primary cross-sectional modality used to evaluate mediastinal masses. MR is typically reserved for specific problem solving and is most useful for: (1) assessing lesions in patients who cannot receive iodinated contrast; (2) likely vascular lesions; (3) confirming the cystic nature of lesions that have high attenuation due to proteinacious contents; and (4) distinguishing thymic hyperplasia from thymic neoplasms. PET is used to confirm increased metabolic activity in suspected malignancy, to assess response of mediastinal tumors to therapy, particularly lymphoma, and to distinguish residual or recurrent tumor from fibrosis (Table 11.1).

For the purposes of the following discussion, the mediastinum is divided into three compartments: anterior (prevascular), middle (visceral), and posterior (paravertebral) compartments, as described in Chapter 10.

Anterior (Prevascular) Mediastinal Masses (Table 11.2)

Vascular Structures. Perhaps the most common thoracic inlet mass is seen in older patients as tortuous arterial structures, in particular the confluence of the right brachiocephalic and right subclavian arteries or left subclavian artery bulging laterally into the upper lobe to produce a thoracic inlet mass (Fig. 11.1). Since the "mass" is situated anteriorly in the thoracic inlet, its lateral border above the clavicle is indistinct, whereas masses that are posterior or paravertebral in location are sharply outlined by apical lung which extends higher posteriorly than anteriorly. This finding is termed the "thoracic inlet" or "cervicothoracic" sign, and helps localize thoracic inlet masses, thereby suggesting the etiology of such lesions. Tortuous arterial structures may be identified by the presence of atherosclerotic calcification, and can often be seen on a lateral chest radiograph as a "mass" projecting posterior to the tracheal air column which is sharply outlined posteriorly. In contrast to other masses in the thoracic inlet, a tortuous vessel is usually associated with tracheal deviation toward the side of the mass, whereas most goiters and other inlet masses displace the trachea contralaterally.

An uncommon vascular cause of an anterior mediastinal or prevascular mass is an aneurysm arising from the right sinus of Valsalva or an ascending aortic aneurysm extending anteriorly. Sinus of Valsalva aneurysms are typically seen incidentally on cardiac CT or MR and not detected radiographically. A prevascular mass arising from the ascending aorta as seen on lateral chest radiography that contains curvilinear calcification should suggest an ascending aortic aneurysm or foregut cyst as potential causes.

Thyroid Masses. In a small percentage of patients with a cervical thyroid goiter, a thyroid carcinoma, or an enlarged gland from thyroiditis, extension of the thyroid through the thoracic inlet into the superior mediastinum may occur. These lesions are usually discovered as incidental findings on chest radiography; a minority of patients will present with complaints of dyspnea or dysphagia as a result of tracheal or esophageal compression respectively. Thyroid goiters, either uninodular or multinodular, arise from the lower pole of the thyroid or thyroid isthmus and can enter the superior mediastinum anterior to the trachea (80% of cases) or to the right and posterolateral to the trachea (20% of cases). In a very small minority of patients with intrathoracic goiter, the connection of the intrathoracic component of the goiter to the cervical gland is a thin fibrous band or is absent and therefore not obvious on cross-sectional imaging.

On chest radiography, an anterosuperior mediastinal mass typically deviates the trachea contralaterally and either posteriorly (anterior masses) or anteriorly (posterior masses). Coarse, clumped calcifications are common in thyroid goiters. Radioiodine studies should be performed as the initial imaging procedure, although false-negative results do occur. CT usually shows characteristic findings: (1) well-defined margins;

TABLE 11.1

UTILITY OF IMAGING MODALITIES IN EVALUATION OF MEDIASTINAL MASSES

MODALITY	UTILITY	LIMITATIONS
Conventional radiography	■ Ready availability ■ Low radiation dose ■ Global assessment of chest ■ Compartmentalization of mass	
Multi-detector CT	■ High contrast resolution ■ Ready availability ■ Detection of calcification ■ Superior spatial resolution to MR	Ionizing radiation Iodinated contrast
Magnetic resonance imaging	■ Iodinated contrast contraindicated ■ Vascular lesions ■ Confirms cysts (foregut, pericardial) ■ Thymic mass vs. hyperplasia	Inability to detect Ca^{++} Lower spatial resolution than CT
FDG-PET	■ Measures metabolic activity ■ Distinguishes necrosis/fibrosis from viable tumor ■ Global assessment of regional/distant metastases ■ Assess treatment response	

TABLE 11.2

ANTERIOR (PREVASCULAR) MEDIASTINAL MASSES

Common	
Vascular	■ Tortuous/dilated brachiocephalic/ right subclavian artery
Thyroid	■ Colloid nodule ■ Goiter
Parathyroid	■ Adenoma
Lymphatic	■ Lymphoma • Hodgkin • Non-Hodgkin ■ Metastatic disease
Thymic	■ Thymoma ■ Thymic hyperplasia
Germ cell neoplasm	■ Teratoma (benign)
Mesenchymal tumors	■ Lipoma
Uncommon	
Vascular	■ Ascending aortic aneurysm ■ Sinus of Valsalva aneurysm
Thyroid	■ Carcinoma
Parathyroid	■ Hyperplasia ■ Carcinoma
Lymphatic	■ Lymphangioma ■ Inflammatory
Thymic	■ Thymic cyst ■ Thymolipoma ■ Thymic neuroendocrine tumor (carcinoid) ■ Thymic carcinoma
Germ cell neoplasm	■ Teratoma (malignant) ■ Seminoma ■ Endodermal sinus tumor ■ Embryonal cell carcinoma ■ Choriocarcinoma
Mesenchymal tumors	■ Leiomyoma ■ Fibroma ■ Hemangioma ■ Hamartoma

(2) continuity of the mass with the cervical thyroid; (3) coarse calcifications; (4) cystic or necrotic areas; (5) baseline high CT attenuation (because of intrinsic iodine content); and (6) intense enhancement (>25 H) as a result of the hypervascularity of most thyroid masses and prolonged enhancement (resulting from active uptake of iodine from contrast media) following intravenous contrast administration (Fig. 11.2). MR is useful in depicting the longitudinal extension of thyroid goiters without the use of intravenous contrast.

Parathyroid Masses. In approximately 2% of patients, the parathyroid glands fail to separate from the thymus in the neck and descend with the gland into the anterosuperior mediastinum. These glands can be found near the thoracic inlet in or about the thymus. This becomes important in the small percentage of patients with persistent clinical and biochemical evidence of hyperparathyroidism following routine neck exploration and parathyroidectomy. Most of these ectopic parathyroid lesions are small (<3 cm) adenomas; rarely, they represent hyperplastic glands or parathyroid carcinoma. When US fails to localize a lesion in the neck, CT, MR, or technetium^{99} sestamibi (Tc-99m-sestamibi) scanning may be useful in detecting mediastinal lesions (Fig. 11.3).

Lymphangiomas. These uncommon masses are tumors comprised of dilated lymphatic channels. The cystic or cavernous form (cystic hygroma) is most commonly discovered in infancy and is often associated with chromosomal abnormalities, including Turner syndrome and trisomies 13, 18, and 21. In infants, these lesions tend to extend from the neck into the anterior mediastinum; less commonly they may arise primarily within the anterior mediastinum in older patients.

Thymomas (Thymic Epithelial Neoplasms). Thymoma is the second most common primary mediastinal neoplasms in adults after lymphoma. These lesions are neoplasms that arise from thymic epithelium with varying numbers of intermixed lymphocytes. Thymic epithelial neoplasms are divided into *thymomas*, in which the neoplastic component reflects thymic epithelial cells, and *thymic carcinomas*, in which the epithelial component shows signs of overt atypia. The World Health

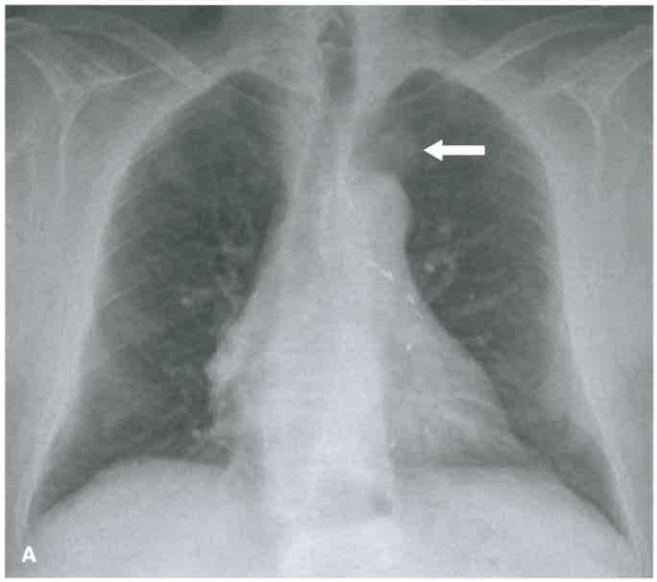

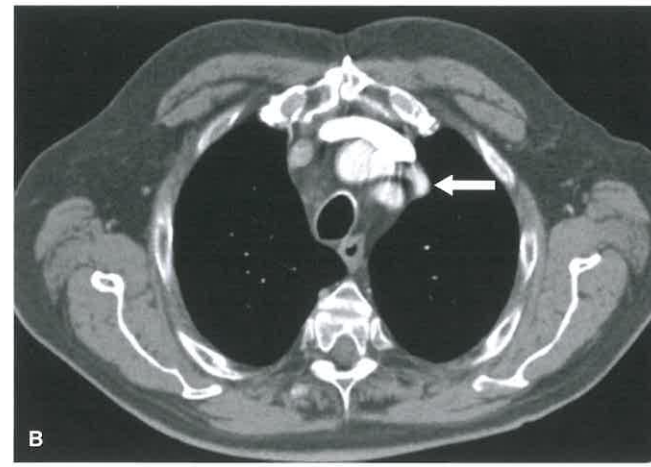

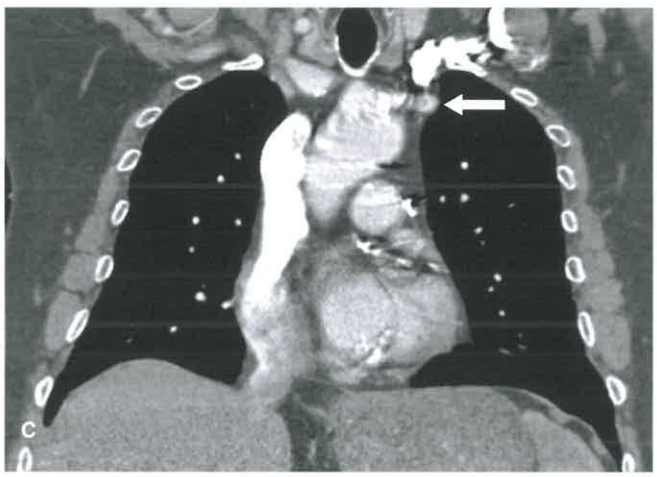

FIGURE 11.1. **Tortuous Left Common Carotid Artery Producing Superior Mediastinal "Mass." A:** Chest radiograph demonstrates a left superior mediastinal mass (*arrow*). **B** and **C:** Axial (**B**) and coronal (**C**) contrast-enhanced scans show a tortuous left common carotid artery arising from the aortic arch (*arrows* in **B** and **C**) as producing the "mass."

Organization classifies these neoplasms based upon the morphology of the epithelial component and the ratio of epithelial cells to lymphocytes. The classification system divides these neoplasms into types A, AB, B1, B2, B3, and C, with a spectrum of histologic changes ranging from the classic encapsulated thymoma (A), which has a favorable prognosis, to thymic carcinoma (C), which generally carries a poor prognosis. For the staging of thymic epithelial neoplasms, the International Thymic Malignancy Interest Group (ITMIG) has developed a detailed classification system based on TNM descriptors.

The average age at diagnosis of thymoma is 45 to 50; these lesions are rare in patients under the age of 20. While most often associated with myasthenia gravis, thymoma has been associated with other paraneoplastic syndromes such as pure red cell aplasia and hypogammaglobulinemia. Of patients with myasthenia gravis, 10% to 15% have a thymoma, while a larger percentage of patients with thymoma (30% to 50%) have or will develop myasthenia. Autoimmune diseases that have been associated with thymoma include Grave disease and lupus.

On chest radiography, thymomas are seen as round or oval, smooth or lobulated soft tissue masses arising near the origin of the great vessels at the base of the heart. CT is best for characterizing thymomas and detecting local invasion preoperatively (Fig. 11.4). As a result of their firm consistency, thymomas characteristically maintain their shape where they contact the sternum anteriorly and heart and great vessels posteriorly. Compared to type A tumors, higher-grade thymomas, particularly types B3 and C, tend to show larger size, more irregular margins, heterogeneous enhancement, regions of necrosis, mediastinal nodal metastases, and calcification. Invasion of tumor through the thymic capsule is present in 33% to 50% of patients (Fig. 11.5). In the majority of these patients, microscopic capsular invasion cannot be determined on CT or MR. Local invasion of mediastinal pleura, pericardium, lung, chest wall, diaphragm, and great vessels occurs in decreasing order of frequency in a minority of patients. Contiguity of a thymoma with the adjacent chest wall or mediastinal structures cannot be used as reliable evidence of invasion of these structures. Drop metastases to dependent portions of the pleural space are a recognized route of spread of thymoma that has invaded the pleura. Extrathoracic metastases are rare, although transdiaphragmatic spread of a pleural tumor into the retroperitoneum has been described. For these reasons, it is important to image the entire thorax and upper abdomen in any patient with suspected invasive disease.

In patients with myasthenia gravis who are being evaluated for thymoma, CT can demonstrate tumors that are not visible on conventional radiography. However, very small thymic tumors may not be distinguishable from a normal or hyperplastic gland with CT, particularly in younger patients with a large amount of residual thymic tissue.

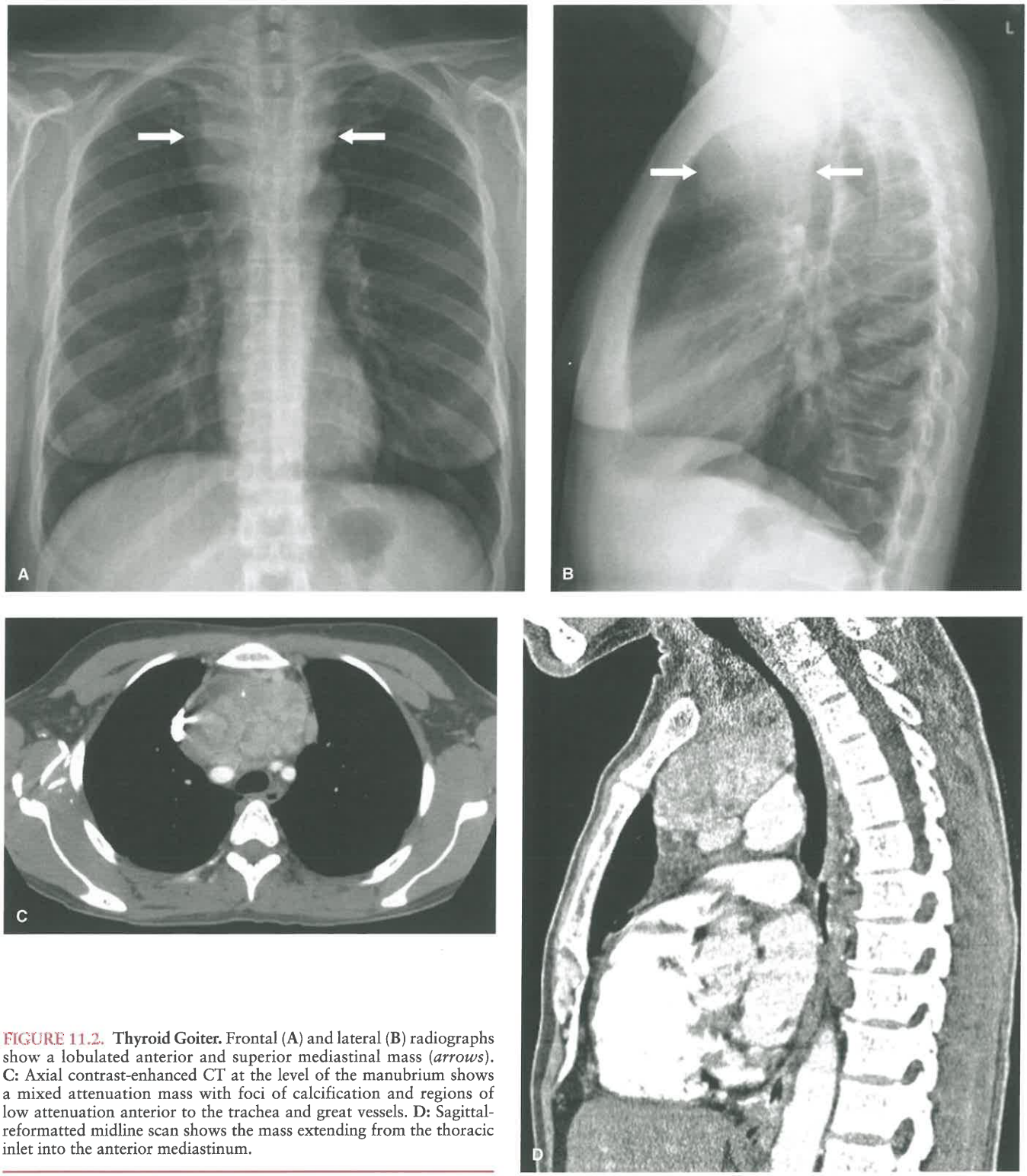

FIGURE 11.2. **Thyroid Goiter.** Frontal (**A**) and lateral (**B**) radiographs show a lobulated anterior and superior mediastinal mass (*arrows*). **C:** Axial contrast-enhanced CT at the level of the manubrium shows a mixed attenuation mass with foci of calcification and regions of low attenuation anterior to the trachea and great vessels. **D:** Sagittal-reformatted midline scan shows the mass extending from the thoracic inlet into the anterior mediastinum.

Thymic cysts may be congenital or acquired. Congenital unilocular thymic cysts are rare lesions that represent remnants of the thymopharyngeal duct and contain thin or gelatinous fluid. They are characterized histologically by an epithelial lining, with thymic tissue in the cyst wall, which distinguishes thymic cysts histologically from other congenital cystic lesions within the anterior mediastinum. Acquired multilocular thymic cysts are postinflammatory in nature and have been associated with AIDS, prior radiation or surgery, and autoimmune conditions such as Sjögren syndrome, myasthenia gravis, and aplastic anemia; in these latter conditions, clinical and radiologic distinction of multilocular thymic cyst from cystic thymoma may be difficult; in fact, the two conditions can coexist. Large cysts will be evident as masses on conventional radiography, and CT or MR will demonstrate the cystic nature of the lesion. If the distinction between a true thymic cyst, cystic degeneration of a thymoma or lymphoma, germ cell neoplasm, or lymphangioma is impossible

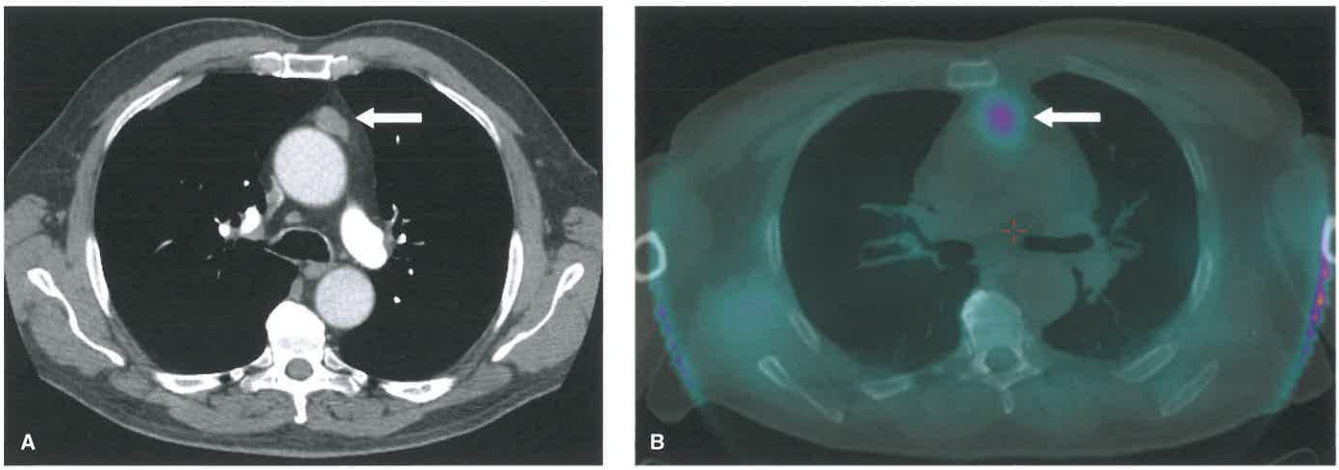

FIGURE 11.3. **Parathyroid Adenoma. A:** Axial contrast-enhanced CT through the upper chest in a 60-year-old male with hypercalcemia demonstrates a preaortic nodule (*arrow*). **B:** Fused SPECT-CT Tc-99m-sestamibi shows increased activity within the lesion (*arrow*). Surgical exploration confirmed an ectopic parathyroid adenoma.

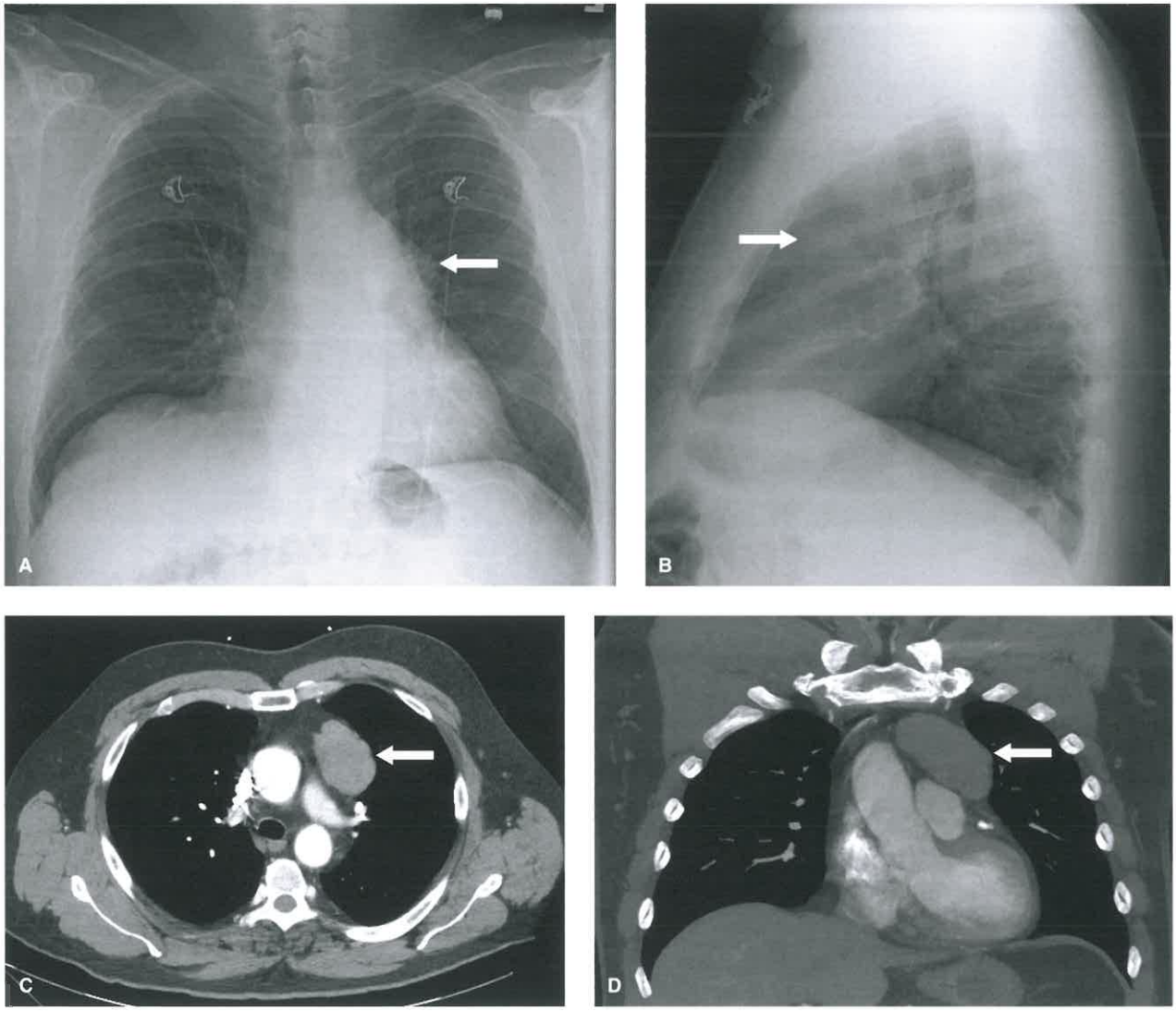

FIGURE 11.4. **Noninvasive Thymoma. A:** Chest radiograph shows a left anterior mediastinal mass (*arrow* in **A**). **B:** Lateral radiograph confirms the anterior location of the mass (*arrow*). **C, D:** Axial (**C**) and maximum intensity coronal (**D**) contrast-enhanced CT scan shows a lobulated left anterior mediastinal mass (*arrows* in **C, D**). Surgical resection revealed a noninvasive thymoma.

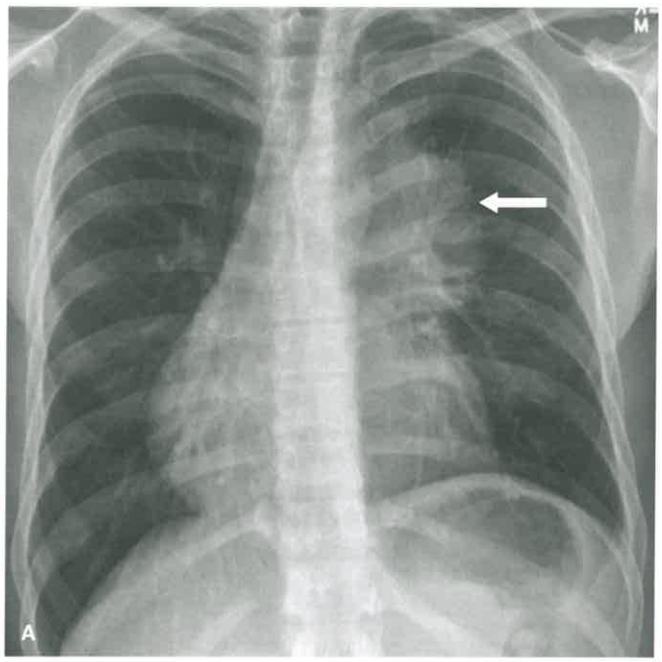

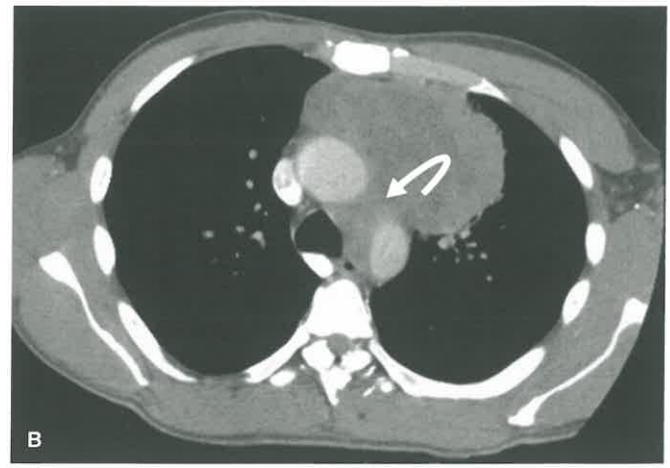

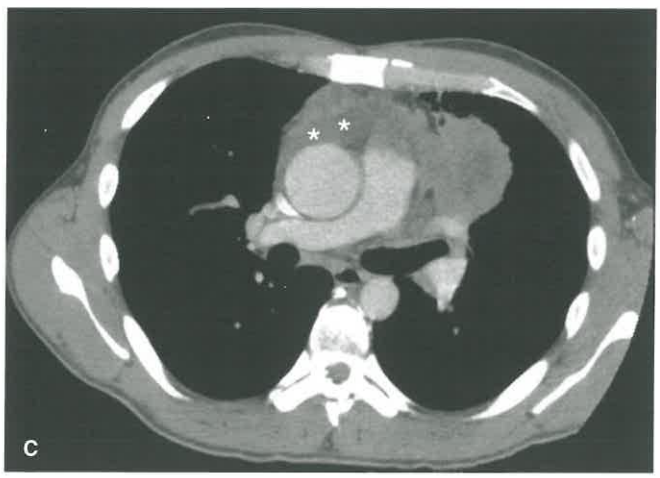

FIGURE 11.5. **Invasive Thymoma. A:** Posteroanterior chest radiograph reveals a left mediastinal mass (*arrow*) with an irregular lateral border. **B:** CT confirms a solid left anterior mediastinal mass (*arrow*) with foci of necrosis. Note soft tissue infiltration of the aortopulmonary window (*curved arrow*) indicating mediastinal invasion. **C:** Axial scan more inferiorly shows broad mediastinal contact by the tumor with associated pericardial effusion (*asterisks*). Mediastinal and pericardial invasion were confirmed at surgery.

on clinical and radiologic grounds, the lesion should be biopsied or resected.

Thymolipoma is a rare, benign thymic neoplasm that consists primarily of fat with intermixed rests of normal thymic tissue. These masses are asymptomatic and therefore are typically large when first detected. Chest radiographs show a large anterior mediastinal mass that, because of its pliable nature, tends to envelope the heart and diaphragm. CT demonstrates a fatty mass with interspersed soft tissue densities. Resection is curative.

Thymic Carcinoid. Neuroendocrine tumors of the thymus are rare malignant neoplasms believed to arise from thymic cells of neural crest origin (amine precursor uptake and decarboxylation [APUD] or Kulchitsky cells). The most common histologic type is carcinoid tumor, which, as with similar lesions arising within the bronchi, ranges in differentiation and behavior from typical carcinoid to atypical carcinoid to small cell carcinoma. Approximately 40% of patients have Cushing syndrome as a result of adrenocorticotropic hormone secretion by the tumor. These patients tend to have smaller lesions at the time of diagnosis since they present early with signs of corticosteroid excess. The carcinoid syndrome associated with thymic carcinoid is uncommon. This lesion is indistinguishable from thymoma on plain radiographs and CT scans.

Thymic Hyperplasia is defined as enlargement of a thymus that is normal on gross and histologic examination. This rare entity occurs primarily in children as a rebound effect in response to an antecedent stress, discontinuation of chemotherapy, or treatment of hypercortisolism. An association with Grave disease has also been noted. The term *thymic hyperplasia* has been used incorrectly to describe the histologic findings of lymphoid follicular hyperplasia of the thymus, found in 60% of patients with myasthenia gravis. In contrast to most cases of true thymic hyperplasia, lymphoid hyperplasia does not produce thymic enlargement. Most patients with thymic hyperplasia have normal sized or diffusely enlarged glands on CT (Fig. 11.6); occasionally thymic hyperplasia will present as a mass that is radiographically indistinguishable from thymoma. Most cases can be resolved by noting a decrease in size on follow-up studies, thereby obviating the need for biopsy. Chemical shift MR with in- and out-of-phase sequences can distinguish hyperplasia, which shows signal decrease on out-of-phase chemical shift imaging due to the presence of microscopic fat within hyperplastic tissue, from thymic neoplasms that do not decrease in signal intensity.

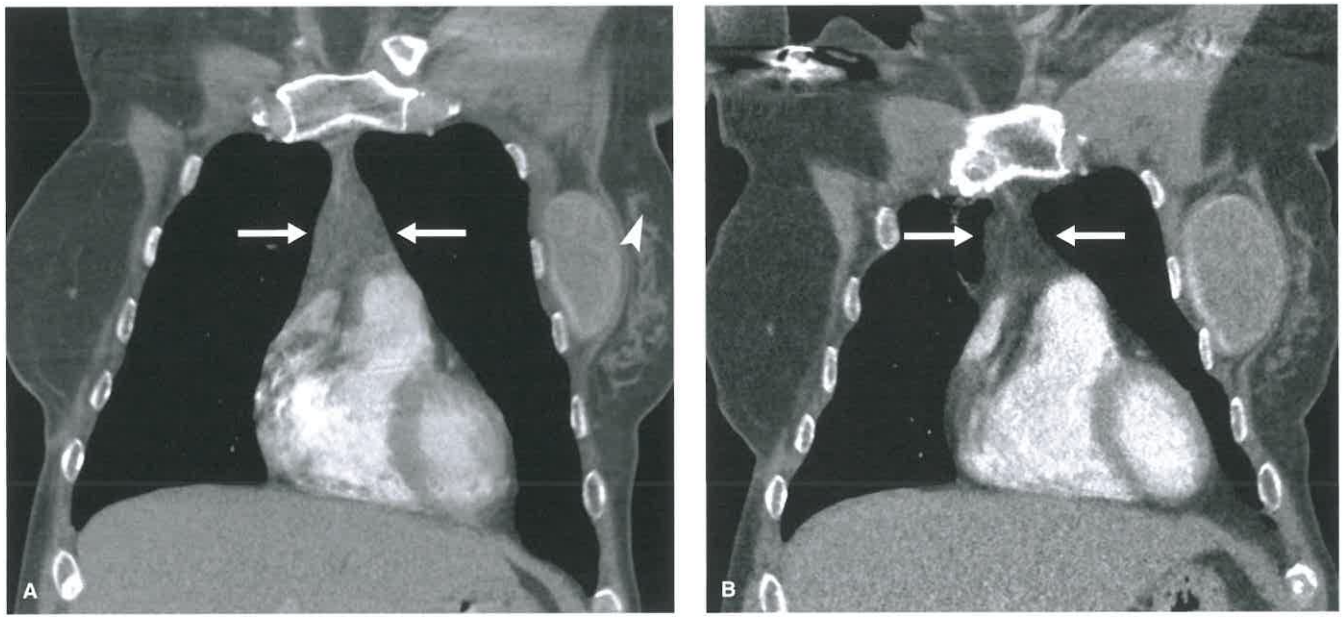

FIGURE 11.6. **Thymic Hyperplasia. A:** Coronal contrast-enhanced CT through the anterior mediastinum in a 55-year-old woman who recently completed chemotherapy for left breast cancer shows a diffusely enlarged thymus (*arrows*) with predominantly soft tissue attenuation. Note left breast prosthesis (*arrowhead*). **B:** Coronal CT scan years later following completion of chemotherapy shows a decrease in size of the thymus (*arrows*) with almost uniform fat attenuation.

Thymic Lymphoma. The thymus is involved in 40% to 50% of patients with the nodular sclerosing subtype of Hodgkin disease. Its radiographic appearance is indistinguishable from that of other solid neoplasms arising within the thymus. The presence of lymph node enlargement in other portions of the mediastinum or anterior chest wall involvement should suggest the diagnosis.

Lymphoma. Hodgkin disease or NHL is the most common primary mediastinal neoplasm in adults. Hodgkin disease involves the thorax in 85% of patients at the time of presentation. The majority (90%) of patients with intrathoracic involvement have mediastinal lymph node enlargement; this most commonly involves the anterior mediastinal and hilar nodal groups. The anterior mediastinum is the most frequent site of a localized nodal mass in patients with Hodgkin disease, particularly those with the nodular sclerosing type (Fig. 11.7). Isolated enlargement of mediastinal or hilar nodes outside the anterior mediastinum should suggest an alternative diagnosis. Only 25% of patients with Hodgkin lymphoma have disease limited to the mediastinum at the time of diagnosis. NHL involves the thorax in approximately 40% of patients at presentation. In contrast to Hodgkin disease, only 50% of patients with NHL and intrathoracic disease have mediastinal nodal involvement, and only 10% of NHL patients have disease that is limited to the mediastinum. Of the various subtypes of NHL that present with mediastinal masses, lymphoblastic lymphoma and diffuse large B-cell lymphoma are the most common (Fig. 11.8). Lymphoma involving a single mediastinal or hilar nodal group is much more common in NHL than in Hodgkin disease. NHL most commonly involves middle mediastinal and hilar lymph nodes; juxtaphrenic and posterior mediastinal nodal involvement is uncommon but is seen almost exclusively in NHL. Patterns of pulmonary parenchymal involvement in lymphoma are discussed in Chapter 13.

While Hodgkin disease spreads in a fairly predictable pattern from one nodal group to an adjacent group, NHL is felt to be a multifocal disorder in which patterns of involvement are unpredictable. Localized intrathoracic Hodgkin disease is usually treated with radiation therapy, with 90% response rates. More widespread Hodgkin disease and NHL are treated with chemotherapy, with better response rates for Hodgkin disease than for NHL.

On conventional radiography, lymphoma involving the anterior mediastinum is indistinguishable from thymoma or germ cell neoplasm and presents as a lobulated mass projecting to one or both sides of the mediastinum (Fig. 11.7). Calcification in untreated lymphoma is extremely uncommon, and its presence within an anterior mediastinal mass should suggest another diagnosis. Involvement of other lymph node stations in the mediastinum, hila, neck, or axilla makes lymphoma more likely. An enlarged spleen displacing the gastric air bubble medially, seen in the upper abdominal portion of the frontal chest radiograph, provides an additional clue to the diagnosis.

MDCT is performed in virtually all patients with lymphoma. The advantages of chest CT include the ability to better characterize and localize masses seen on chest radiographs; detection of subradiographic sites of involvement that can alter disease staging, prognosis, and therapy; guidance for transthoracic or open biopsy; the ability to monitor response to therapy; and detection of relapse. The appearance of nodal involvement in lymphoma varies; most commonly, discrete enlarged solid lymph nodes or conglomerate masses of nodes are seen (Fig. 11.7C). Parenchymal involvement is usually the result of direct extranodal extension of a tumor from hilar nodes along the bronchovascular lymphatics; this is better appreciated on CT than on chest radiography. Likewise, a tumor extending from the mediastinum to the pericardium, subpleural space, and chest wall is best appreciated on CT or MR. On MR, untreated lymphoma appears as a mass of uniform low signal intensity on T1WIs and uniform high signal intensity or intermixed areas of low and high signal intensity on T2WIs. The areas of low signal intensity on T2WIs of untreated patients may be a result of foci of fibrotic tissue in nodular sclerosing Hodgkin disease.

Patients with successfully treated mediastinal Hodgkin disease often have residual soft tissue density in the affected

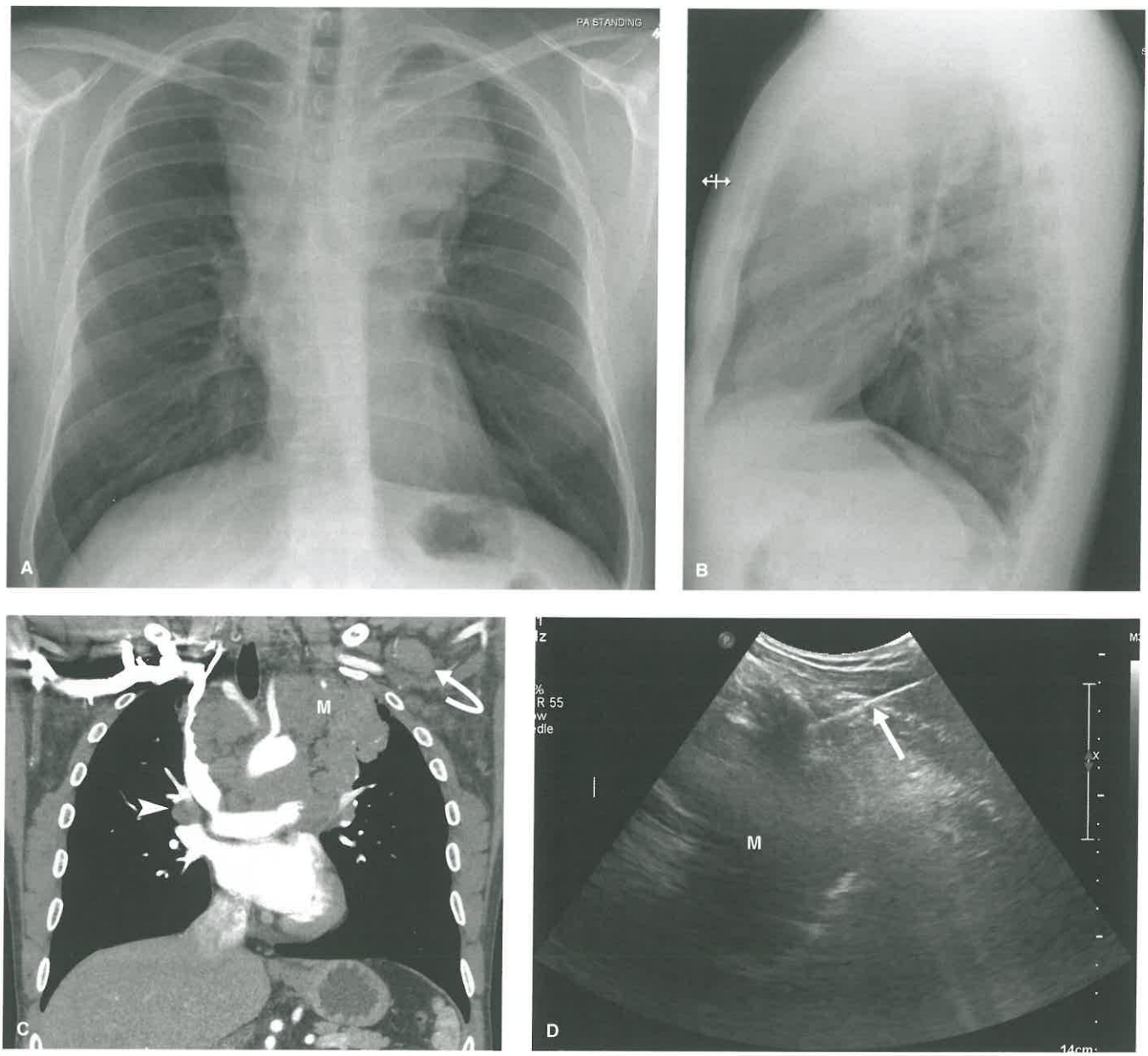

FIGURE 11.7. **Hodgkin Lymphoma. A, B:** Posteroanterior (**A**) and lateral (**B**) chest radiographs in a 35-year-old man shows a large, lobulated anterior and superior mediastinal mass. **C:** Coronal contrast-enhanced CT at the level of the aortic arch shows a large superior mediastinal mass (M) encompassing the arch and great vessels. Note enlarged right hilar (*arrowhead*) and left axillary (*curved arrow*) lymph nodes. **D:** Ultrasound-guided core needle biopsy shows the mass (M) with biopsy needle (*arrow*) at edge of lesion. Core biopsy demonstrated nodular sclerosing subtype of Hodgkin disease.

mediastinal compartments, with dystrophic calcification commonly seen within treated nodes (Fig. 11.9). CT and fluorodeoxyglucose (FDG)-PET are used to monitor the response of lymphoma to therapy. While CT can accurately assess tumor regression and detect relapse within nodal groups outside the treated region, the ability to distinguish residual tumor from sterilized fibrotic masses is limited. Residual soft tissue masses have been reported in up to 50% of patients, most commonly with nodular sclerosing Hodgkin disease, and are more common when the pretreatment mass is large. Some patients with residual masses on CT or MR will have tumor recurrence within 6 to 12 months after the completion of therapy. In general, the appearance of high signal intensity regions on T2WIs more than 6 months after treatment should suggest recurrence. FDG-PET is clearly superior to CT or MR in distinguishing recurrent tumor from fibrosis in both Hodgkin disease and NHL.

Germ Cell Neoplasms, which include teratoma, seminoma, choriocarcinoma, endodermal sinus tumor, and embryonal cell carcinoma, arise from collections of primitive germ cells that arrest in the anterior mediastinum on their journey to the gonads during embryologic development. Since they are histologically indistinguishable from germ cell tumors arising in the testes and ovaries, the diagnosis of a primary malignant mediastinal germ cell neoplasm requires exclusion of a primary gonadal tumor as a source of mediastinal metastases. A key in distinguishing primary from metastatic mediastinal germ cell neoplasm is the presence of retroperitoneal lymph node involvement in metastatic gonadal tumors.

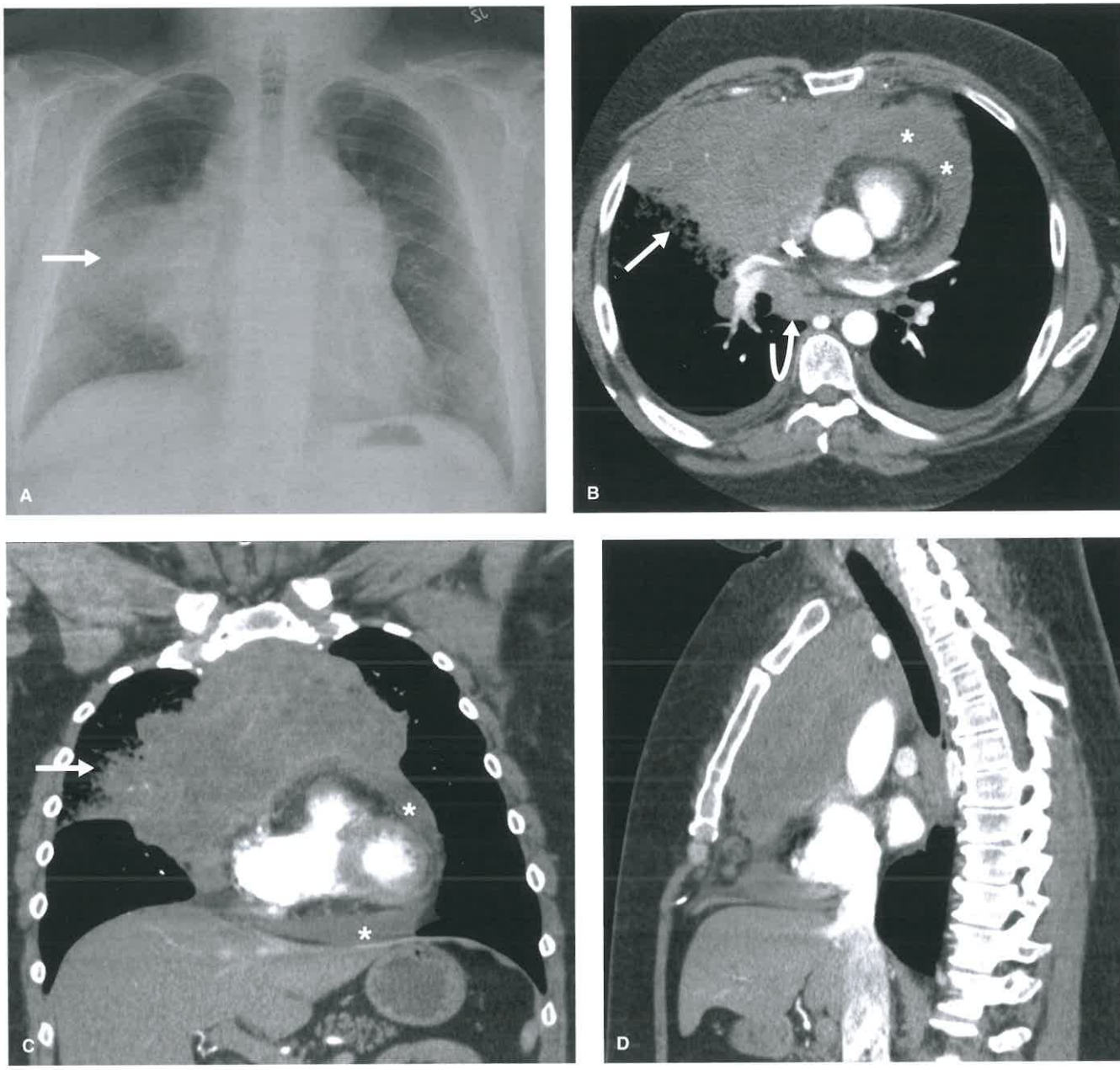

FIGURE 11.8. **Non-Hodgkin Lymphoma, Diffuse Large B-Cell Type. A:** Chest radiograph shows a mediastinal mass extending into the right perihilar lung (*arrow*). **B, C, D:** Axial (**B**), coronal (**C**), and sagittal (**D**) contrast-enhanced CT scan shows a large anterior mediastinal mass with mixed attenuation extending into the right upper lobe (*arrows* in **B** and **C**) with associated right hilar and subcarinal lymph node enlargement (*curved arrows*) small pleural effusions and a pericardial effusion (*asterisks* in **B** and **C**). Core needle biopsy showed diffuse large B-cell lymphoma.

The most common benign mediastinal germ cell neoplasm is teratoma, comprising 60% to 70% of mediastinal germ cell neoplasms. Teratomas may be cystic or solid. Cystic or mature teratoma is the most common type of teratoma seen in the mediastinum; these lesions commonly contain tissues of ectodermal, mesodermal, and endodermal origin. Solid germ cell tumors are usually malignant, with seminoma comprising 25% to 50% of such lesions. Most germ cell neoplasms are detected in patients 20 to 40 years of age. While benign tumors have a slight female preponderance (female/male, 60%/40%), malignant tumors are seen almost exclusively in males.

Radiographically, these tumors have an appearance similar to thymoma. While the majority are located in the anterior mediastinum, up to 10% are found in the posterior mediastinum. Benign lesions are often round or oval and smooth in contour; an irregular, lobulated, or ill-defined margin suggests malignancy. Calcification is present in 33% to 50% of tumors but is nonspecific unless in the form of a tooth. On CT, benign teratomas are usually cystic and may contain soft tissue, bone, teeth, fat, or, rarely, fat-fluid levels (Fig. 11.10). Malignant teratoma, seminoma, choriocarcinoma, and endodermal sinus (yolk sac) tumors are malignant lesions seen primarily in young men. Seminoma is the most common malignant germ cell neoplasm, accounting for 30% of these tumors. The radiographic findings are nonspecific. CT typically shows a large lobulated soft tissue mass that may contain areas of

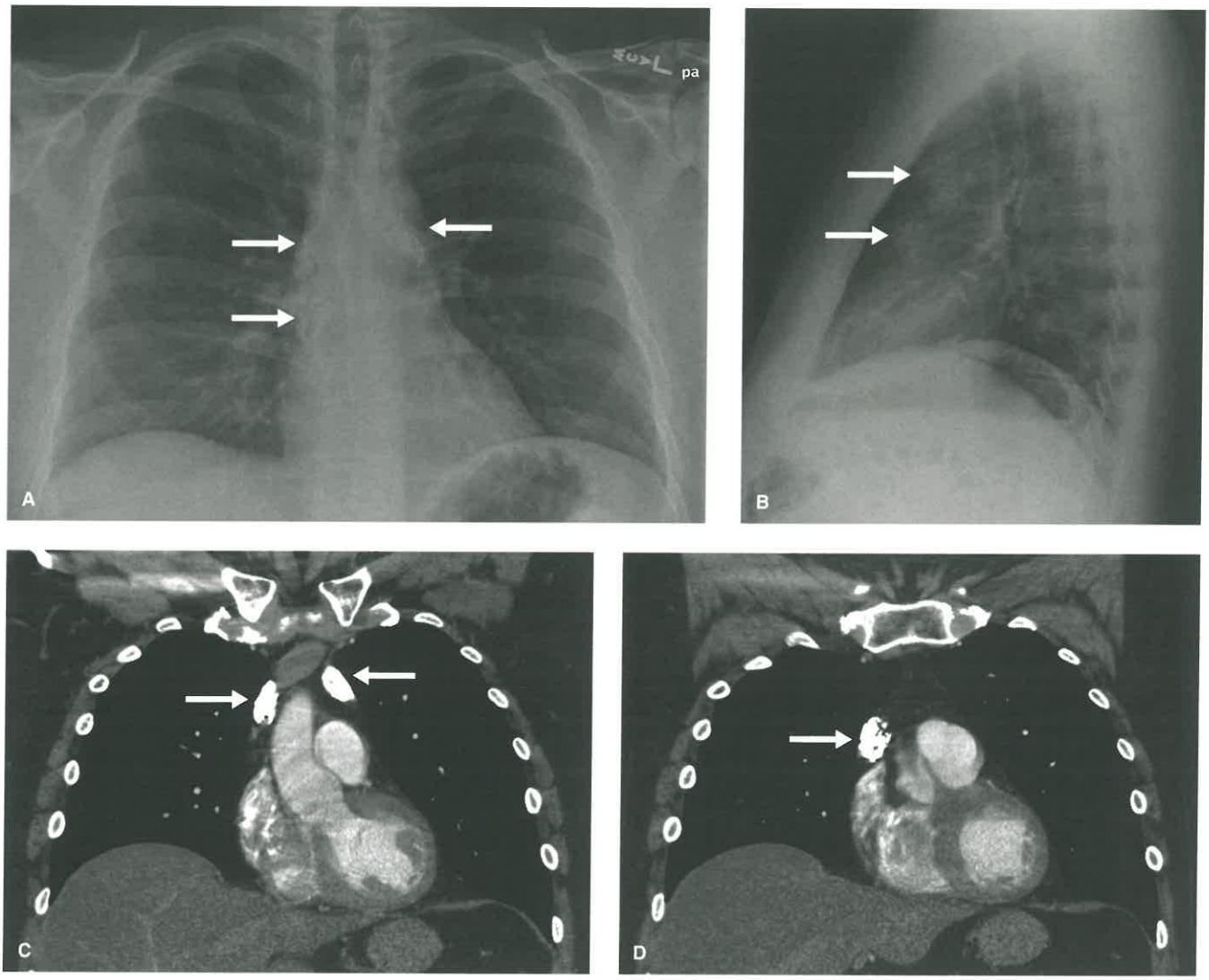

FIGURE 11.9. **Treated Hodgkin Lymphoma With Residual Calcified Nodes. A, B:** Chest radiographs in frontal (**A**) and lateral (**B**) projections demonstrate coarse anterior and superior mediastinal calcification (*arrows*). **C, D:** Contrast-enhanced coronal CT scans through the anterior mediastinum (**C, D**) show multiple calcified nodes (*arrows*) reflecting treated tumor.

hemorrhage, calcification, or necrosis (Fig. 11.11). Elevated serum levels of human chorionic gonadotropin (beta-HCG) or alpha-fetoprotein (alpha-FP) are helpful in the diagnosis of suspected malignant mediastinal germ cell neoplasm, while clinical or CT evidence of gynecomastia is an additional clue to diagnosis.

Mesenchymal Tumors. Benign and malignant tumors arising from the fibrous, fatty, muscular, or vascular tissues of the mediastinum may present as mediastinal masses, most commonly in the anterior mediastinum. Lipomas can occur in any location in the mediastinum but are most often anterior. The diagnosis is made by recognition of a well-defined mass of uniform fatty attenuation (under –50 HU). The presence of soft tissue elements should raise the possibility of a thymolipoma or liposarcoma (Fig. 11.12); the latter may show evidence of invasion of adjacent structures at the time of diagnosis. Fat within a mature teratoma or transdiaphragmatic herniation of omental fat is usually easily distinguished from a lipoma.

Hemangiomas are benign tumors composed of vascular channels and may be associated with the syndrome of hereditary hemorrhagic telangiectasia. A pathognomonic sign on chest radiographs is the recognition of phleboliths within a smooth or lobulated soft tissue mass. Angiosarcomas are rare malignant vascular neoplasms that are indistinguishable from other invasive neoplasms arising within the anterior mediastinum.

Leiomyomas are rare benign neoplasms that arise from smooth muscles within the mediastinum. Similarly, fibromas and hamartomas (tumors that contain more than one mesenchymal element) can rarely present as anterior mediastinal masses.

Middle (Visceral) Mediastinal Masses (Table 11.3)

Lymphatic/Lymph Node Enlargement and Masses. Most middle mediastinal lymph node masses are malignant, representing metastases from lung cancer, extrathoracic malignancy, or lymphoma. Benign causes of middle mediastinal lymph node enlargement include foregut cysts, vascular anomalies or

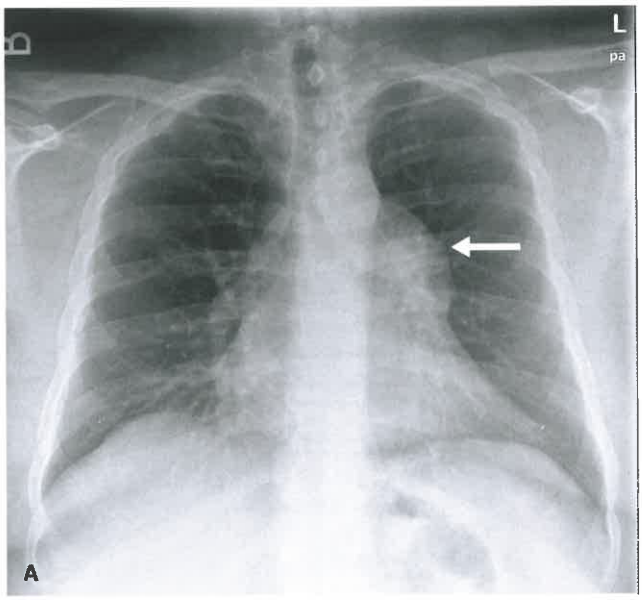

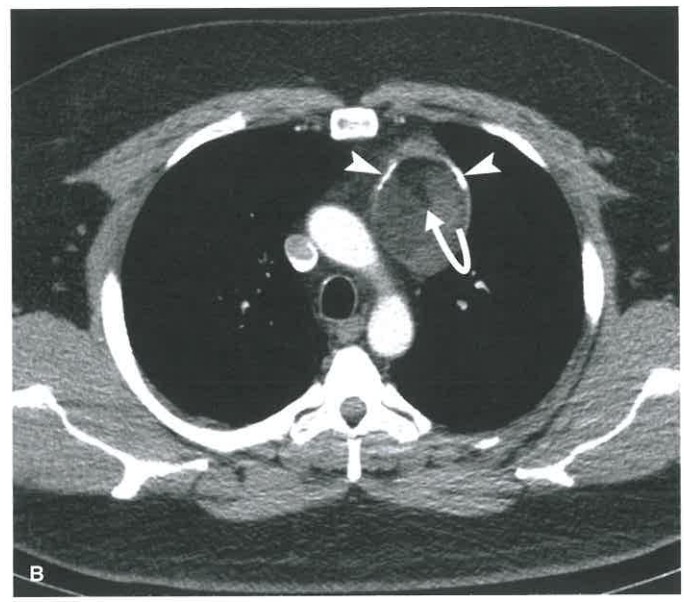

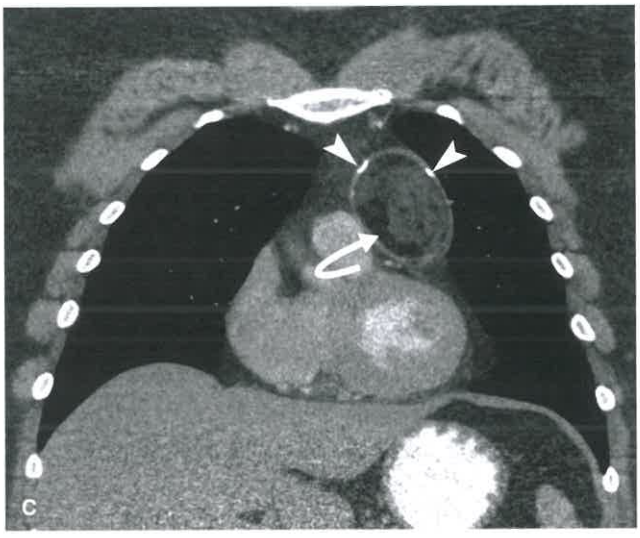

FIGURE 11.10. **Mature Teratoma. A:** Frontal chest radiograph in a 42-year-old man shows a left mediastinal mass (*arrow*). **B, C:** Axial (B) and coronal-reformatted (C) contrast-enhanced CT in a reveals a rounded anterior mediastinal mass with peripheral calcification (*arrowheads* in B and C) containing fat (*curved arrow* in B and C) and soft tissue elements. Surgical resection confirmed **a** mature teratoma.

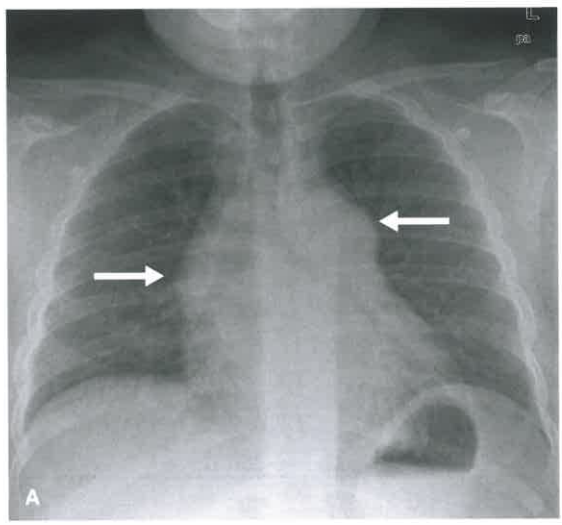

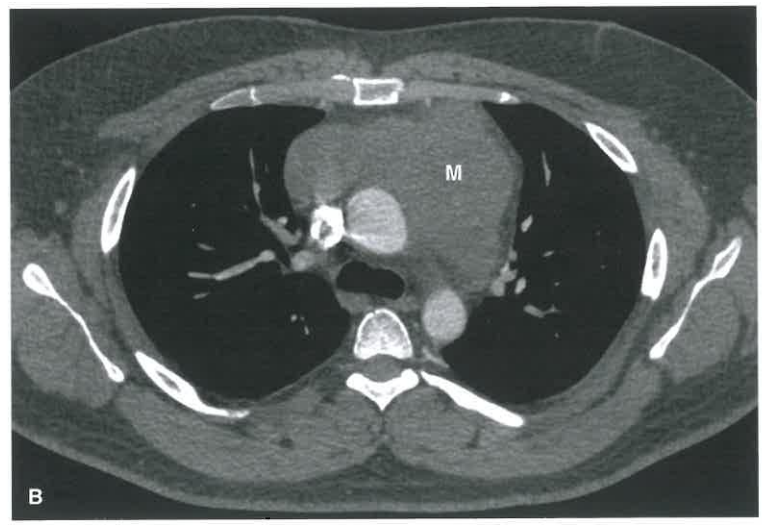

FIGURE 11.11. **Malignant Nonseminomatous Germ Cell Tumor. A:** Posteroanterior chest radiograph in a 30-year-old man reveals a mediastinal mass (*arrows*). **B:** Axial contrast-enhanced CT demonstrates a lobulated anterior mediastinal soft tissue mass (M). CT-guided biopsy showed a nonseminomatous tumor with mixed yolk sac and embryonal elements.

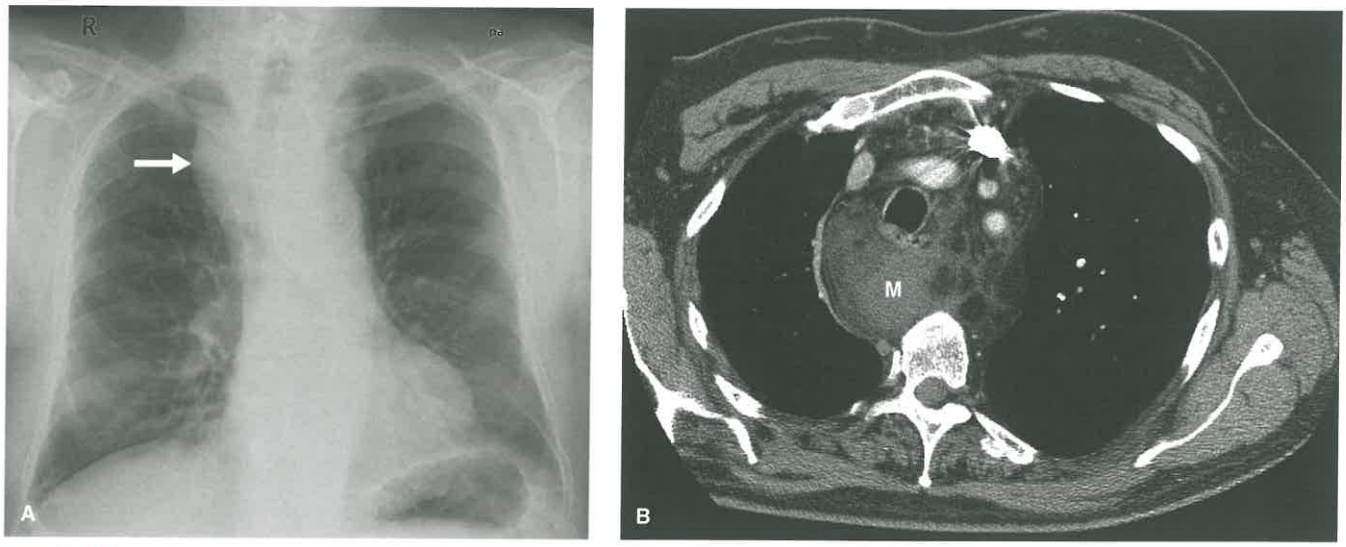

FIGURE 11.12. **Liposarcoma of Mediastinum. A:** Frontal chest radiograph in an 83-year old man with dysphagia shows a superior mediastinal mass (*arrow*). **B:** Contrast-enhanced axial CT shows a mixed attenuation mass (M) with fatty and soft tissue elements infiltrating the mediastinum. CT-guided biopsy showed a liposarcoma confirmed at surgery.

aneurysms (Fig. 11.13), sarcoidosis, mycobacterial and fungal infection, and angiofollicular lymph node hyperplasia (Castleman disease).

On conventional radiography, several findings suggest that a middle mediastinal mass represents lymph node enlargement. The presence of multiple bilateral mediastinal masses that distort the lung/mediastinal interface is relatively specific for lymph node enlargement. Occasionally, calcification can be detected within enlarged lymph nodes on plain radiographs; CT is more sensitive in detecting nodal calcification and its distribution within lymph nodes.

One of the prime indications for performing thoracic CT is to detect the presence of enlarged mediastinal lymph nodes. CT is most often obtained to confirm an abnormal chest radiographic finding or to evaluate a patient with suspected mediastinal disease despite normal radiographs (a patient with a suspicious solitary pulmonary nodule or with cervical Hodgkin disease). MDCT allows for the recognition of abnormally enlarged lymph nodes that would not be evident on chest radiography. In general, abnormal lymph nodes are seen as round or oval soft tissue masses that measure >1.0 cm in their short-axis diameter. Although CT is unable to distinguish between benign inflammatory nodes and those involved by malignancy based upon size criteria alone, CT can provide useful information about the internal density of the nodes (Table 11.4). A standardized classification system for hilar and mediastinal lymph nodes is the International Association for the Study of Lung Cancer (IASLC) lymph node map, which is used with the eighth edition of the TNM classification system for lung cancer. This lymph node classification system, based upon the Mountain-Dressler American Thoracic Society lymph node map, groups intrathoracic lymph nodes into stations

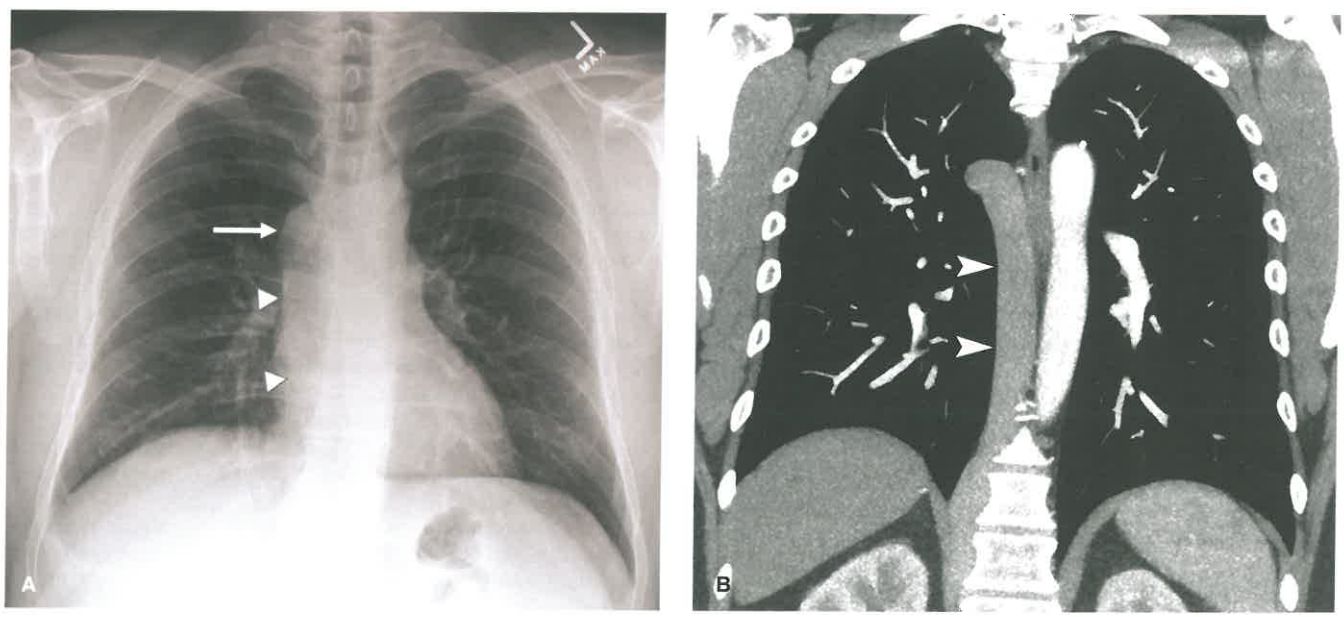

FIGURE 11.13. **Azygos Continuation of the Inferior Vena Cava (IVC) as Right Paratracheal Mass. A:** Frontal chest radiograph in an asymptomatic 40-year-old man demonstrates a right paratracheal mass (*arrow*), contiguous with a vertically oriented tubular opacity (*arrowheads*). **B:** Coronal contrast-enhanced CT shows a dilated azygos vein (*arrowheads*). The intrahepatic IVC (not shown) was absent; no other anomalies were identified.

TABLE 11.3

MIDDLE (VISCERAL) MEDIASTINAL MASSES

Lymphatic	Malignancy	■ Primary intrathoracic malignancy • Non–small cell carcinoma • Small cell carcinoma • Primary pulmonary lymphoma • Carcinoid tumor • Extrathoracic malignancy with nodal spread ■ Head and neck CA ■ Breast CA ■ Genitourinary (renal cell, seminoma) ■ Melanoma ■ Systemic malignancy • Lymphoma • Leukemia (T cell) • Kaposi sarcoma
	Inflammatory	■ Infection • Mycobacterial ■ Tuberculosis • Fungal ■ Histoplasmosis ■ Coccidioidomycosis ■ Blastomycosis • Viral ■ Measles ■ Mononucleosis ■ Granulomatous • Sarcoidosis ■ Other • Castleman disease
Cyst		■ Foregut cyst • Bronchogenic cyst • Enteric cyst • Neurenteric cyst ■ Mesothelial cyst • Pericardial cyst
Tracheal/ central bronchial malignancy		■ Carcinoid tumor ■ Salivary gland tumor • Mucoepidermoid CA • Adenoid cystic CA ■ Bronchogenic carcinoma • Squamous cell carcinoma • Small cell carcinoma
Vascular		■ Thoracic aortic aneurysm ■ Double aortic arch ■ Dilated azygos vein ■ Dilated main pulmonary artery ■ Esophageal varices
Esophageal		■ Neoplasms • Leiomyoma • GIST • Carcinoma ■ Diverticula ■ Hiatal hernia

TABLE 11.4

CT DENSITY OF MEDIASTINAL/HILAR LYMPH NODES

■ DENSITY	■ PATTERN	■ CONDITION
Calcification	Central or punctate	■ Mycobacterial ■ Fungal ■ Amyloidosis ■ Sarcoidosis ■ Silicosis ■ Mycobacterial infection ■ Treated lymphoma
	Peripheral (EGGSHELL)	
	Complete	
Hypervascular		■ Carcinoid tumor ■ Small cell carcinoma ■ Metastases • Renal cell carcinoma • Thyroid carcinoma ■ Castleman disease
Necrosis		■ Infection • Mycobacterial • Fungal • Whipple disease (Tropheryma whipplei) ■ Metastases • Squamous cell carcinoma • Seminoma • Lymphoma

and correlates with easily identifiable CT and anatomic landmarks. The IASLC lymph node mapping system can be found in Chapter 13, Figure 13.19.

In addition to the detection and characterization of enlarged mediastinal nodes, CT can help guide diagnostic nodal tissue sampling. This is usually most helpful in the setting of suspected bronchogenic carcinoma, where accurate staging of mediastinal nodal disease is important for prognostic purposes and treatment planning. The detection of enlarged lymph nodes on CT may suggest biopsy via endobronchial ultrasound (EBUS), endoscopic ultrasound (EUS), or mediastinoscopy.

As mentioned above, mediastinal lymph node enlargement is common in Hodgkin disease and NHL. Lymphoma accounts for 20% of all mediastinal neoplasms in adults, and most patients with intrathoracic lymphoma have concomitant extrathoracic disease. In most patients, the nodal enlargement is bilateral but asymmetric (Fig. 11.14). Nodular sclerosing Hodgkin disease commonly results in lymph node enlargement, predominantly within the anterior mediastinum and thymus. Isolated posterior nodal enlargement is usually seen only in patients with NHL.

Leukemia, particularly the T-lymphocytic varieties, can cause intrathoracic lymph node enlargement. The lymph node enlargement is usually confined to the middle mediastinal and hilar nodes.

The most common source of metastases to middle mediastinal nodes is lung cancer. In the majority of patients, symptoms or radiographic findings suggest the presence of a primary tumor in the lung. In a small percentage of patients, particularly those with small cell carcinoma, the primary carcinoma may be inconspicuous or invisible on conventional radiography, with nodal metastases being the only visible abnormality

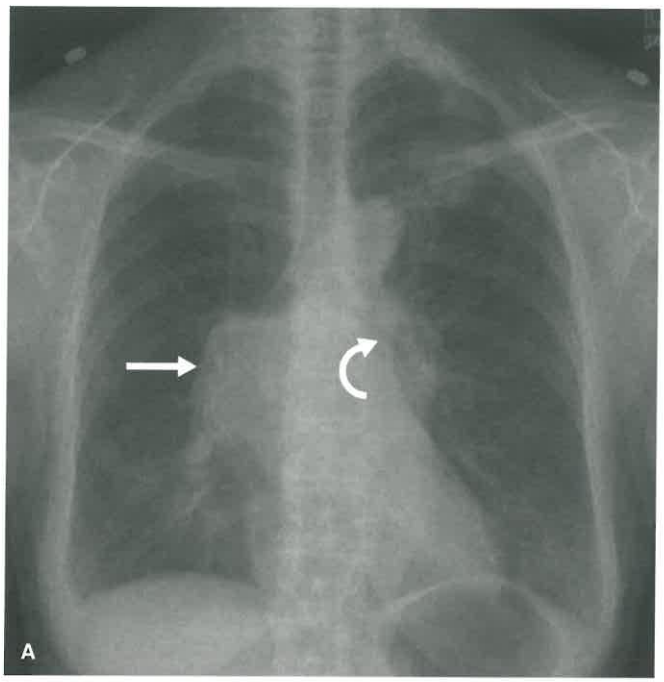

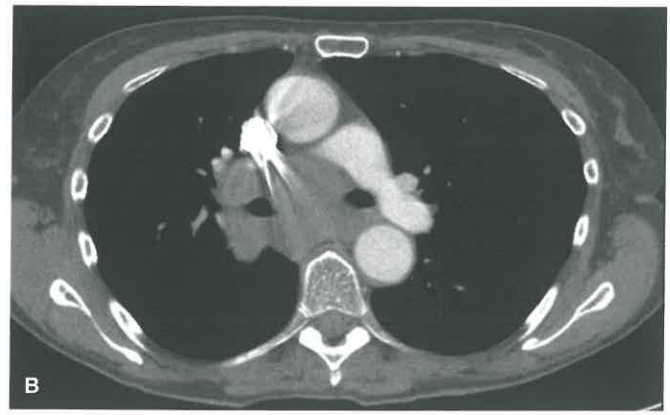

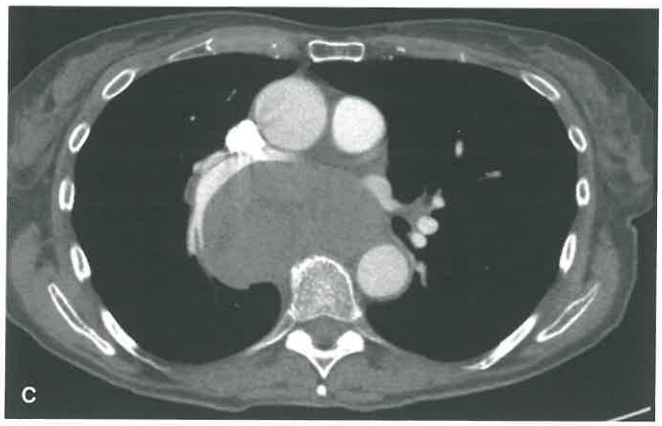

FIGURE 11.14. **Right Hilar/Middle Mediastinal Mass due to Non-Hodgkin Lymphoma. A:** Chest radiograph shows a right hilar and subcarinal mass (*arrow*). Note splaying of the carina and narrowing of the left main bronchus (*curved arrow*). The density overlying the left upper lobe is an artifact. **B** and **C:** Axial contrast-enhanced CT scans show a right hilar and subcarinal soft tissue mass. CT-guided core biopsy of the subcarinal component revealed non-Hodgkin lymphoma.

(Fig. 11.15). Lymph node enlargement is often unilateral on the side of the visible pulmonary or hilar abnormality (Fig. 13.20A). Paratracheal and aorticopulmonary nodes are most commonly involved. Since the accuracy of CT in predicting the presence or absence of mediastinal lymph node metastases is approximately 60% to 70%, PET-CT should be performed in virtually all patients with lung cancer for accurate staging. A more thorough discussion of mediastinal nodal involvement in lung cancer may be found in Chapter 13.

Lymph node metastases from extrathoracic malignancies can result in mediastinal node enlargement, either with or without concomitant pulmonary metastases. These mediastinal nodal metastases may result from inferior extension of neck masses (thyroid carcinoma, head and neck tumors); extension along lymphatic channels from below the diaphragm (testicular or renal cell carcinoma, gastrointestinal malignancies); or hematogenous extension (breast carcinoma, melanoma, Kaposi sarcoma).

Mediastinal lymph node enlargement is very common in patients with sarcoidosis, occurring in 60% to 90% of patients at some stage of their disease. Nodal enlargement is typically bilateral and symmetric and involves the hila as well as the mediastinum; this usually allows for differentiation of sarcoidosis from lymphoma and metastatic disease. In sarcoidosis, the enlarged nodes produce a lobulated appearance on chest radiographs and CT, because the enlarged nodes do not coalesce. This is in contrast to lymphoma and nodal metastases, in which the intranodal tumor extends through the nodal capsule to form conglomerate-enlarged nodal masses. Right and left paratracheal lymph nodes are typically involved; anterior or posterior mediastinal nodal enlargement has been described with greater frequency recently, probably as a result of the improved sensitivity of CT as compared to radiography for detecting nodal enlargement in these regions.

A variety of infections, most commonly histoplasmosis, coccidioidomycosis, blastomycosis, and tuberculosis can cause mediastinal nodal enlargement (Fig. 11.16). Typically these patients have parenchymal opacities on chest radiographs, but isolated lymph node enlargement may be seen in primary tuberculosis, particularly in children and young adults. Bacterial infections such as anthrax, bubonic plague, and tularemia are uncommon causes of lymph node enlargement. Typically, there will be signs and symptoms of acute infection, and chest radiographs will show evidence of pneumonia. Bacterial lung abscesses also may be associated with reactive lymph node enlargement. Hilar and mediastinal lymph nodes may be enlarged in patients with measles, pneumonia, and infectious mononucleosis.

Angiofollicular or giant lymph node hyperplasia, known as *Castleman disease (CD)* is a lymphoproliferative disorder characterized by enlargement of hilar and mediastinal lymph

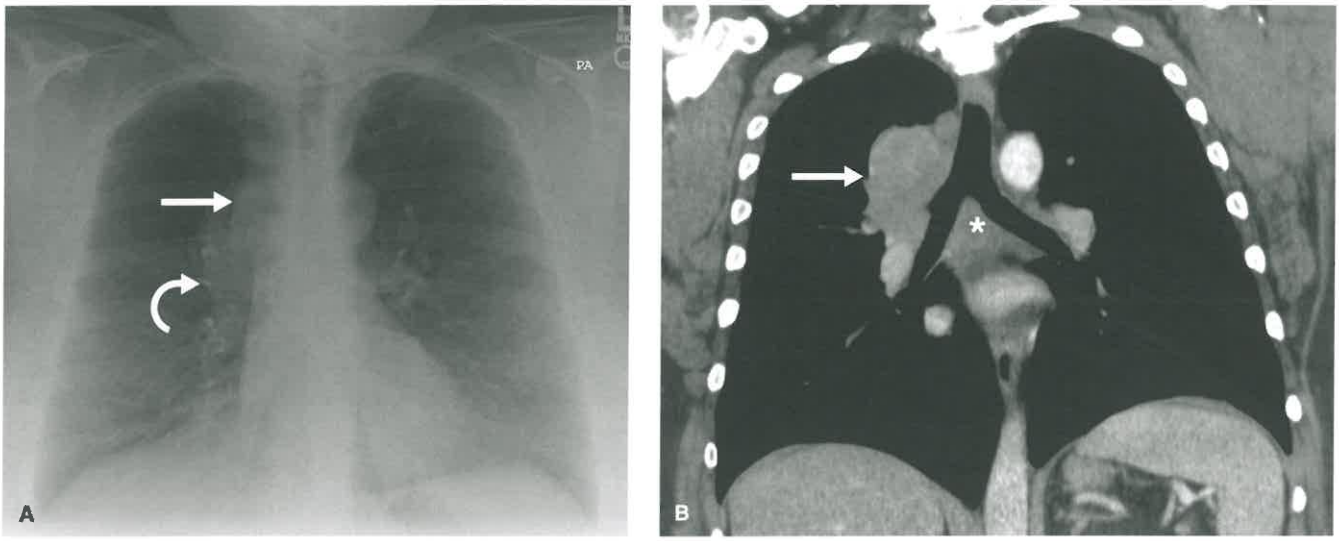

FIGURE 11.15. **Middle Mediastinal/Hilar Lymph Node Enlargement From Small Cell Carcinoma of Lung. A:** Frontal chest radiograph in a 46-year-old man with small cell carcinoma of lung shows right paratracheal (*straight arrow*) and right hilar (*curved arrow*) lymph node enlargement. **B:** Coronal contrast-enhanced CT scan at the level of the tracheal carina shows a lobulated right paratracheal and right hilar soft mass (*straight arrow*) with associated subcarinal lymph node enlargement (*asterisk*).

nodes, predominantly in the middle and posterior mediastinal compartments. The disease can be localized (unicentric or one lymph node group) producing a single group of enlarged lymph nodes or multicentric involving multiple lymph node groups and organs containing lymphatic tissue. The unicentric form of CD has an excellent prognosis whereas multicentric disease is most often associated with HIV and human herpesvirus 8 (HHV-8) infection and has a more variable clinical course. In the more common hyaline vascular subtype, the disease presents as an asymptomatic mediastinal soft tissue mass. The less common plasma cell subtype is associated with multicentric disease and is often associated with systemic symptoms. Histologically, there is replacement of normal nodal architecture with multiple germinal centers and multiple small vessels with hyalinized walls that course perpendicularly toward the germinal centers to give a characteristic "lollipop" appearance on light microscopy. The vascular nature of these masses accounts for the intense enhancement seen on contrast-enhanced CT. Calcification within these masses has been described. Unicentric lesions are cured by resection, whereas multicentric disease associated with HHV-8 infection is treated by rituximab and HHV-8 negative disease with siltuximab.

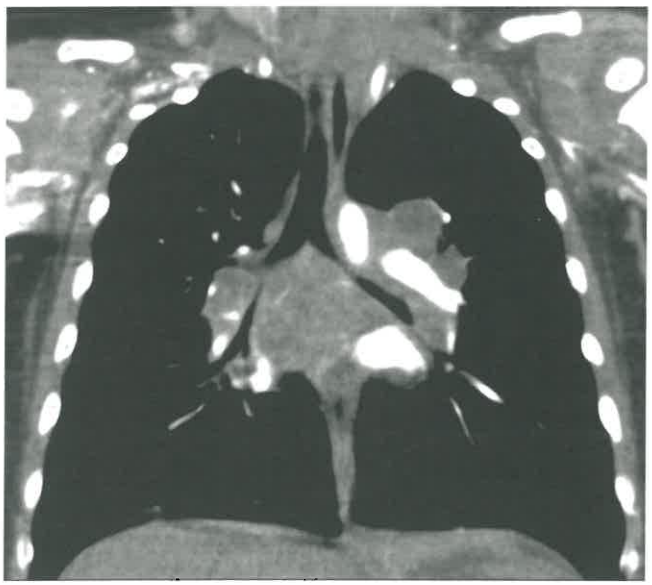

FIGURE 11.16. **Tuberculous Lymph Node Enlargement.** Coronal contrast-enhanced CT at the level of the tracheal carina in a child with primary tuberculosis demonstrates enlarged bilateral hilar and subcarinal lymph nodes with necrosis. Specimens obtained by bronchoscopy revealed *Mycobacterium tuberculosis*.

Foregut and Mesothelial Cysts are common mediastinal lesions that typically present as asymptomatic masses on routine chest radiographs in young adults. CT and MR show findings characteristic of the cystic nature of these lesions.

Bronchogenic cysts result from anomalous budding of the tracheobronchial tree during embryologic development. To be characterized as bronchogenic in origin, the wall of the cyst must be lined by a respiratory epithelium with pseudostratified columnar cells and contain seromucous glands; some may contain cartilage and smooth muscle within their walls. It is often difficult to distinguish between bronchogenic and enteric cysts based on their location and pathologic appearance; the term *foregut cyst* has been used to describe those lesions that cannot be specifically characterized. The majority of bronchogenic cysts (80% to 90%) arise within the mediastinum in the vicinity of the tracheal carina. Most mediastinal lesions are asymptomatic; occasionally, compression of the tracheobronchial tree or esophagus may produce dyspnea, wheezing, or dysphagia. Rarely, mediastinal cysts become secondarily infected after communication with the airway or esophagus, or they cause symptomatic compression after rapid enlargement following hemorrhage. Bronchogenic cysts are seen as soft tissue masses in the subcarinal or right paratracheal space on frontal chest radiographs; less common sites of involvement include the hilum, posterior mediastinum, and periesophageal region. They appear as a single smooth, round, or elliptic mass; a minority are lobulated in contour. MDCT is the method of choice for the diagnosis of a mediastinal cyst. If a well-defined, thin-walled mass of fluid density (0 to 10 H) is seen that fails to enhance following intravenous contrast administration, it can be assumed to represent a benign cyst (Fig. 11.17). High CT attenuation (>40 H) suggesting a solid

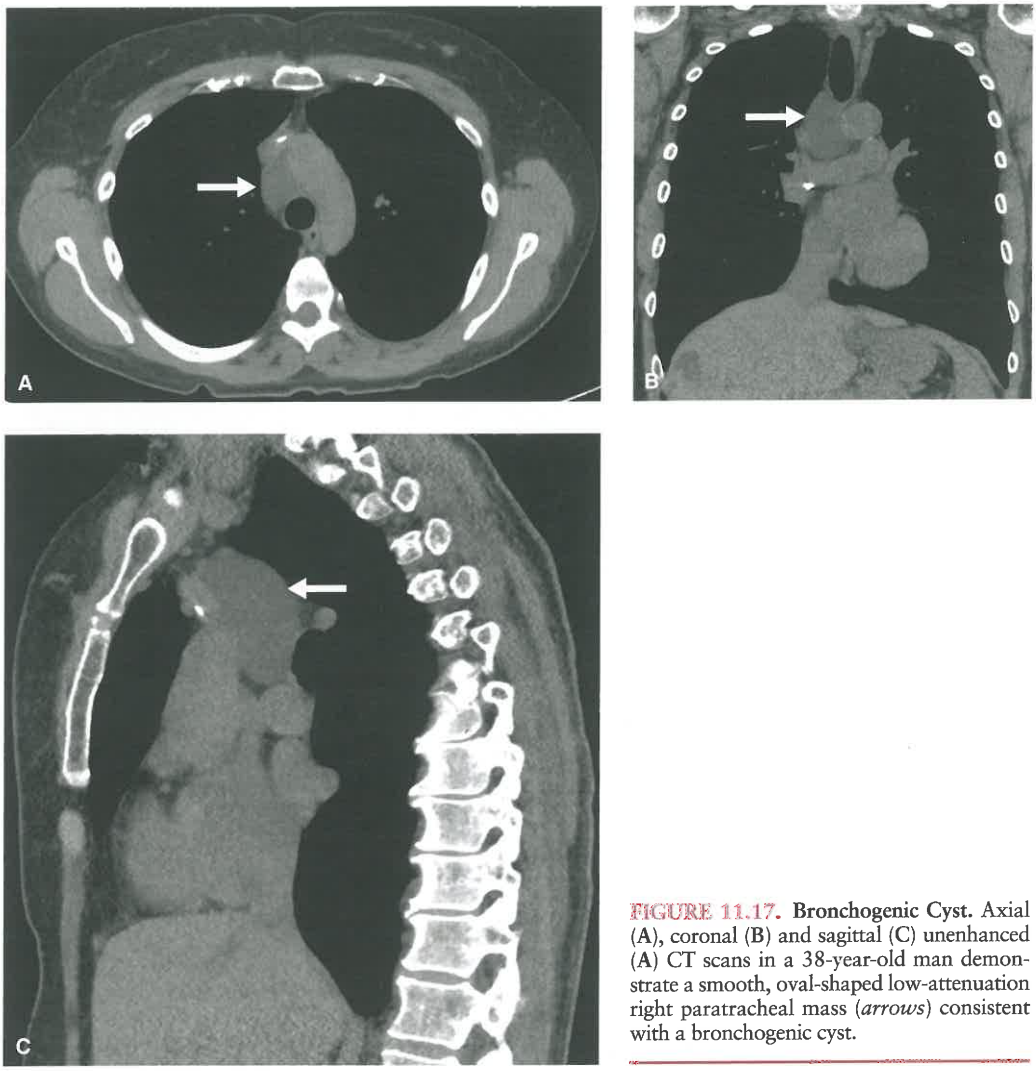

FIGURE 11.17. **Bronchogenic Cyst.** Axial (**A**), coronal (**B**) and sagittal (**C**) unenhanced (**A**) CT scans in a 38-year-old man demonstrate a smooth, oval-shaped low-attenuation right paratracheal mass (*arrows*) consistent with a bronchogenic cyst.

mass can be seen when the cyst is filled with mucoid material, milk of calcium, or blood. Calcification of the cyst wall has been described but is uncommon. MR shows characteristic low signal intensity on T1WIs and high signal intensity on T2WIs. The presence of proteinaceous material within the cyst will shorten T1 relaxation times, yielding high signal intensity on T1WIs; no change in signal will be seen on postcontrast MR studies. While resection is required for definitive diagnosis, most patients with characteristic imaging features who are asymptomatic are managed nonsurgically. Both transbronchoscopic and percutaneous needle aspiration and drainage have been described for diagnosis and treatment of these lesions.

Pericardial cysts arise from the parietal pericardium and contain clear serous fluid surrounded by a layer of mesothelial cells. Most often, they arise in the anterior cardiophrenic angle, with right-sided lesions being twice as common as left-sided lesions; approximately 20% arise more superiorly within the mediastinum. These lesions usually present as incidental asymptomatic round or oval masses in the cardiophrenic angle (Fig. 11.18). Their pliable nature can be demonstrated with a change in patient position. CT typically shows a unilocular cystic mass adjacent to the heart; MR or US via a subxiphoid approach shows findings characteristic of a simple cyst. As with bronchogenic cysts, there have been reports of cysts with high attenuation on CT that on resection are found to be filled with proteinaceous or mucoid material. The differential diagnosis for cardiophrenic angle masses includes pericardial cyst, an enlarged

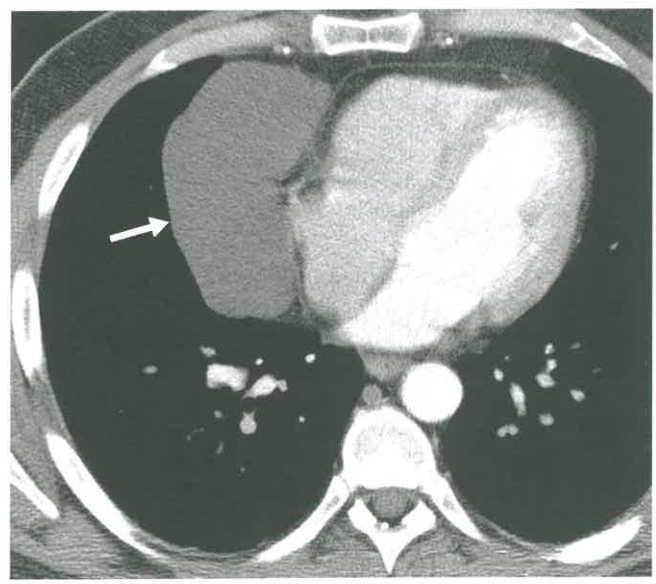

FIGURE 11.18. **Pericardial Cyst.** Enhanced CT scan through heart shows a smooth, sharply marginated, low-attenuation mass (*arrow*) in the right cardiophrenic angle, consistent with a pericardial cyst.

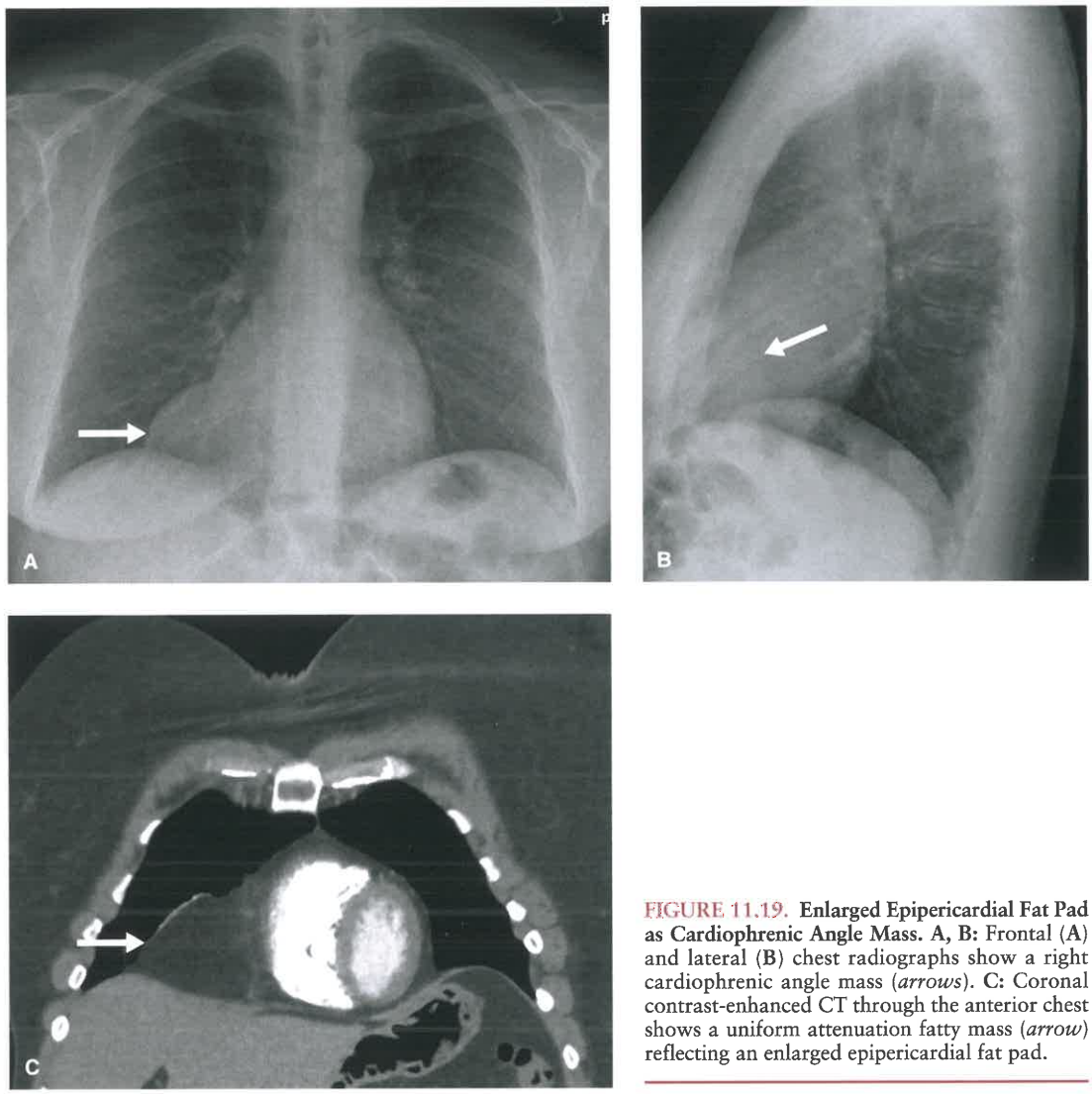

FIGURE 11.19. **Enlarged Epipericardial Fat Pad as Cardiophrenic Angle Mass. A, B:** Frontal (**A**) and lateral (**B**) chest radiographs show a right cardiophrenic angle mass (*arrows*). **C:** Coronal contrast-enhanced CT through the anterior chest shows a uniform attenuation fatty mass (*arrow*) reflecting an enlarged epipericardial fat pad.

epipericardial fat pad (Fig. 11.19), enlarged juxtaphrenic lymph nodes, and diaphragmatic hernias (discussed in Chapter 17).

Tracheal and Central Bronchial Masses commonly produce upper airway symptoms with obstructive pneumonitis and atelectasis and rarely present as asymptomatic mediastinal masses. Occasionally, central airway masses present as radiographic abnormalities when they distort the tracheal air column or mediastinal contour. These masses are discussed in Chapter 15.

Esophageal Lesions. Lesions in the middle or distal third of the esophagus may present as visceral mediastinal masses. Common presenting symptoms include dysphagia and aspiration pneumonia, although many patients are asymptomatic.

The majority of esophageal neoplasms, excluding lesions that arise at the esophagogastric junction, are squamous cell carcinomas. Unlike benign neoplasms of the posterior mediastinum, these lesions, when seen on chest radiographs, are rarely asymptomatic. Typically these patients have a history of dysphagia and significant weight loss. Difficulty in detecting asymptomatic lesions and the absence of a serosa account for the advanced stage of most esophageal carcinoma at presentation and a 5-year survival rate of less than 20%. Patients with esophageal carcinoma may have abnormal radiographic findings which may include abnormal convexity of the azygoesophageal recess, mediastinal widening from the tumor itself or associated esophageal dilatation (distal tumors), thickening of the tracheoesophageal stripe (proximal tumors), and tracheal deviation or narrowing. The diagnosis is usually made on barium esophagram and confirmed by endoscopic biopsy. CT scanning has proved accurate for staging esophageal carcinoma: findings include an intraluminal mass; thickening of the esophageal wall; loss of fat planes between the esophagus and adjacent mediastinal structures (usually the trachea, with upper esophageal lesions, and the descending aorta, with lower esophageal lesions); and evidence of nodal and distant metastases.

Several benign esophageal neoplasms, including leiomyoma and gastrointestinal stromal tumors (GISTs) can present as smooth, solitary mediastinal masses projecting laterally from the posterior mediastinum on frontal chest radiographs. They generally involve the lower third of the esophagus from the level of the subcarinal space to the esophageal hiatus. Initial evaluation is with barium esophagram, which shows a smooth, broad-based mass forming obtuse margins with the esophageal wall. CT demonstrates a smooth, well-defined soft tissue mass adjacent to the esophagus that enhances with intravenous contrast. The smooth nature of these tumors and the absence of esophageal dilatation above the mass helps distinguish benign tumors from carcinoma.

Pulsion diverticula arising at the cervicothoracic esophageal junction or distal esophagus are false diverticula representing

mucosal outpouchings through defects in the muscular layer of the esophagus. A large proximal pulsion diverticulum (Zenker) may extend through the thoracic inlet and appear as a retroesophageal superior mediastinal mass containing an air–fluid level on upright chest radiographs. A distal pulsion diverticulum appears as a juxtadiaphragmatic mass with an air–fluid level projecting to the right of midline. Barium esophagram is diagnostic.

A dilated esophagus resulting from functional (achalasia, scleroderma) or anatomic (stricture, carcinoma) obstruction may produce a mass that courses vertically over the length of the mediastinum, projecting toward the right side on frontal chest radiographs (Fig. 11.20). An air–fluid level on upright films is usually present. A completely air-filled, dilated esophagus appears as a thin curvilinear line along the medial right thorax, because the right lateral wall of the esophagus is outlined by intraluminal air medially and the right lung laterally. An esophagram or CT will confirm the diagnosis of a dilated esophagus; determination of the cause of obstruction often requires endoscopy or occasionally esophageal manometry.

Esophageal varices may produce a round or lobulated retrocardiac mass in patients with portal hypertension. The diagnosis is usually made by endoscopic recognition of submucosal varices involving the distal esophagus. The varices are readily recognized on contrast CT, MR, or portal venography.

A common cause of a mass in the inferior visceral mediastinum is a hiatal hernia. This results from a separation of the superior margins of the diaphragmatic crura and stretching of the phrenoesophageal ligament. The stomach is by far the most common structure in the hernia sac (Fig. 11.21); the gastric cardia (sliding hernia) or fundus (paraesophageal hernia)

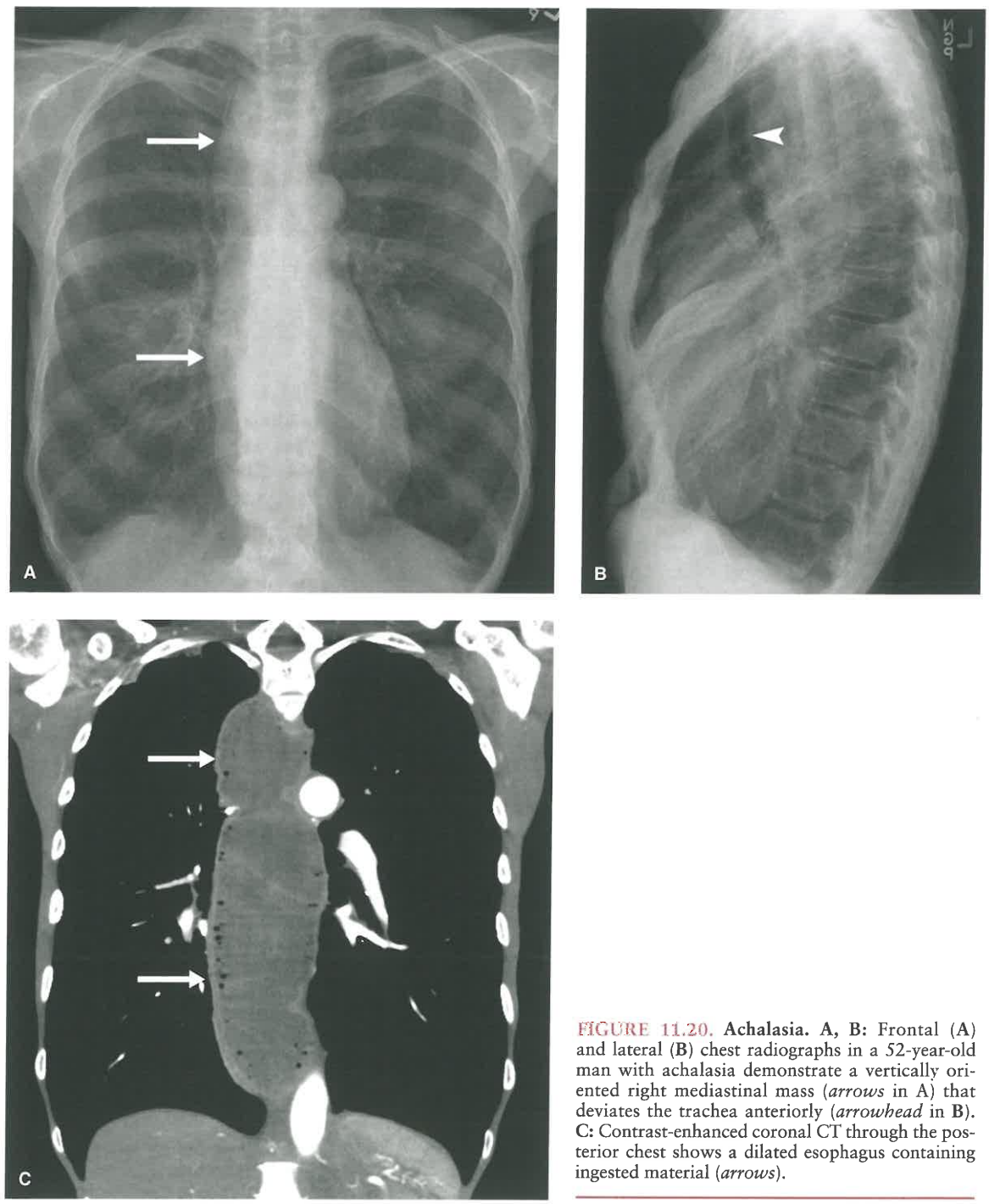

FIGURE 11.20. **Achalasia. A, B:** Frontal (**A**) and lateral (**B**) chest radiographs in a 52-year-old man with achalasia demonstrate a vertically oriented right mediastinal mass (*arrows* in A) that deviates the trachea anteriorly (*arrowhead* in **B**). **C:** Contrast-enhanced coronal CT through the posterior chest shows a dilated esophagus containing ingested material (*arrows*).

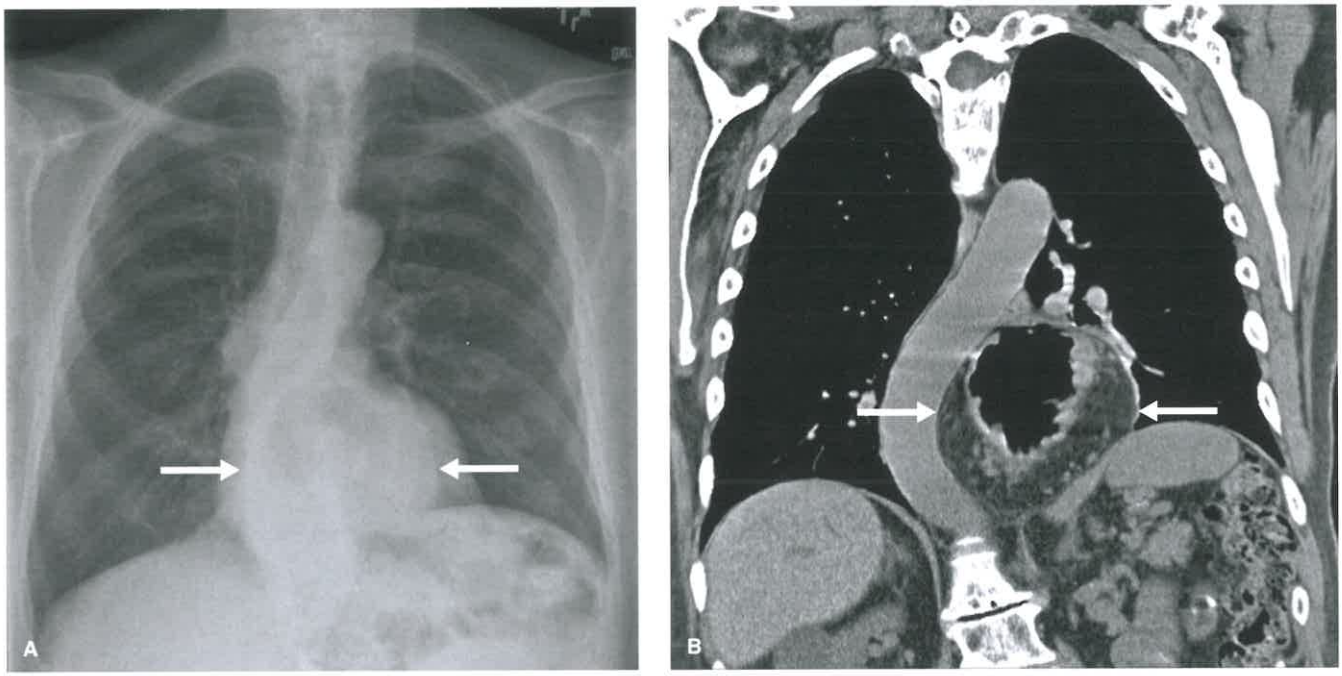

FIGURE 11.21. **Hiatal Hernia. A:** Chest radiograph shows a retrocardiac mass containing air (*arrows*). **B:** Coronal CT scan at the level of the descending aorta shows a hiatal hernia (*arrows*).

may be involved. Rarely, omental fat, ascitic fluid, or a pancreatic pseudocyst herniates through the esophageal hiatus into the mediastinum (Fig. 11.22). The characteristic location at the esophageal hiatus and the presence of a rounded density containing an air or air–fluid level on upright films are diagnostic. Barium esophagram or CT will confirm the diagnosis.

Enteric/Neurenteric Cysts. Enteric cysts are fluid-filled masses lined by enteric epithelium. Esophageal cysts usually arise intramurally or immediately adjacent to the esophagus (Fig. 11.23). When an enteric cyst has a persistent communication with the spinal canal (canal of Kovalevsky) and is associated with congenital defects of the thoracic spine (anterior spina bifida, hemivertebrae, or butterfly vertebrae), it is termed a *neurenteric cyst*. CT or MR can confirm the cystic nature of these masses. If the cyst communicates with the GI tract, it may contain air or an air–fluid level or opacify with contrast during an upper GI series.

Diaphragmatic Hernias, which may present as paracardiac masses, are discussed in Chapter 17.

Vascular Lesions. Congenital or acquired anomalies of the heart and great vessels are common middle mediastinal masses and are discussed in the sections on Pediatric and Cardiac Radiology.

Neurogenic Lesions. Rarely, a neurofibroma arising from the phrenic nerve may present as a middle mediastinal juxtacardiac mass.

Posterior (Paravertebral) Mediastinal Masses (Table 11.5)

Neurogenic Tumors. Posterior mediastinal masses arising from neural elements are classified by their tissue of origin. Three groups have been recognized: (1) tumors arising from intercostal nerves (schwannoma, neurofibroma); (2) sympathetic ganglia (ganglioneuroma, ganglioneuroblastoma, and neuroblastoma); and (3) paraganglionic cells (paraganglionoma). Tumors in each of these three groups may be benign or malignant neoplasms (6). Although neurogenic tumors can occur at any age, they are most common in young patients. Neuroblastoma and ganglioneuroma are most common in children, whereas schwannoma and neurofibroma affect adults more frequently.

Histologically, both schwannoma and neurofibroma are comprised of spindle cells that arise from the Schwann cell. While neurofibroma is an encapsulated tumor that contains interspersed neurons, schwannoma is not encapsulated and contains no neuronal elements. Both tumors are more common in patients with neurofibromatosis. Multiple lesions in the mediastinum, particularly bilateral apicoposterior masses, are virtually diagnostic of neurofibromatosis. A small percentage of schwannomas (10%) are locally invasive (malignant schwannoma).

Radiographically, intercostal nerve tumors appear as round or oval paravertebral soft tissue masses. CT shows a smooth or lobulated paraspinal soft tissue mass, which may erode the adjacent vertebral body or rib (Fig. 11.24). CT demonstration of tumor extension from the paravertebral space into the spinal canal via an enlarged intervertebral foramen is characteristic of a "dumbbell" neurofibroma. MR is the modality of choice for imaging a suspected neurofibroma. In addition to the occasional demonstration of both intra- and extra-spinal canal components, MR of neurofibromas shows typical high signal intensity on T2WIs and often enhances following gadolinium administration.

Tumors that arise from the sympathetic ganglia represent a continuum from the histologically benign ganglioneuroma found in adolescents and young adults to the highly malignant neuroblastoma seen almost exclusively in children under the age of 5. These tumors generally present as elongated, vertically oriented paravertebral soft tissue masses with a broad area of contact with the posterior mediastinum (Fig. 11.25). These findings may help distinguish these lesions from schwannomas or neurofibromas, which usually maintain an acute angle with the vertebral column and posterior mediastinum and therefore tend to show sharp superior and inferior margins on lateral chest radiographs. Large masses may erode vertebral bodies

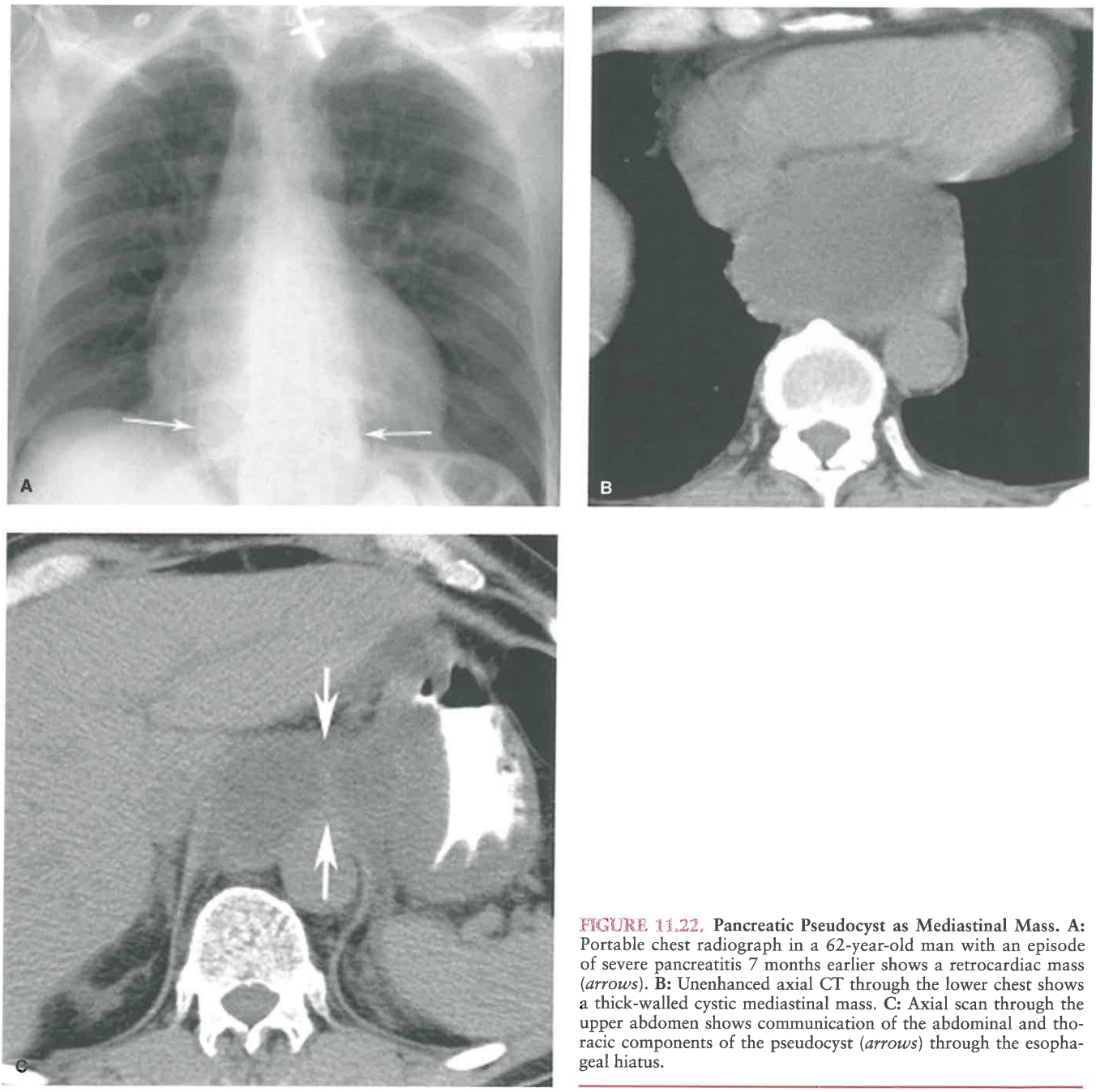

FIGURE 11.22. **Pancreatic Pseudocyst as Mediastinal Mass. A:** Portable chest radiograph in a 62-year-old man with an episode of severe pancreatitis 7 months earlier shows a retrocardiac mass (*arrows*). **B:** Unenhanced axial CT through the lower chest shows a thick-walled cystic mediastinal mass. **C:** Axial scan through the upper abdomen shows communication of the abdominal and thoracic components of the pseudocyst (*arrows*) through the esophageal hiatus.

or ribs. Calcification, seen in up to 25% of cases, is a helpful diagnostic feature of these tumors but does not help distinguish benign from malignant neoplasms. Because these tumors often produce catecholamines, urinary levels of vanillylmandelic acid or metanephrines, which are byproducts of catecholamine metabolism, may be elevated. Prognosis depends upon the histologic features of the tumor and the patient's age and extent of disease at the time of diagnosis.

Mediastinal paragangliomas are tumors that arise from neural crest or chromaffin cells that lie in proximity to the thoracolumbar sympathetic ganglia of the autonomic nervous system. The posterior mediastinum is the site of fewer than 25% of mediastinal paragangliomas, with the majority arising in the anterior or middle mediastinum. Radiographically, these tumors are indistinguishable from other neurogenic tumors. However, most patients have hypertension and biochemical evidence of excess catecholamine production. CT and angiography demonstrates a hypervascular mass. I-123 metaiodobenzylguanidine (MIBG), Ga-68 DOTA (DOTATATE) PET-CT, or F-18-FDG PET-CT can be used to confirm the diagnosis.

Vertebral Abnormalities. A variety of conditions that affect the thoracic spine may manifest as posterior mediastinal masses. These lesions typically produce lateral deviation of the paraspinal reflection on frontal radiographs. Often, the bony origin of these lesions is not obvious on initial examination, making distinction from neurogenic tumors and other posterior mediastinal masses difficult.

Neoplastic, infectious, metabolic, traumatic, or degenerative processes of the thoracic spine may produce a paraspinal mass by one of four mechanisms: (1) expansion of vertebral body or posterior elements (multiple myeloma, aneurysmal

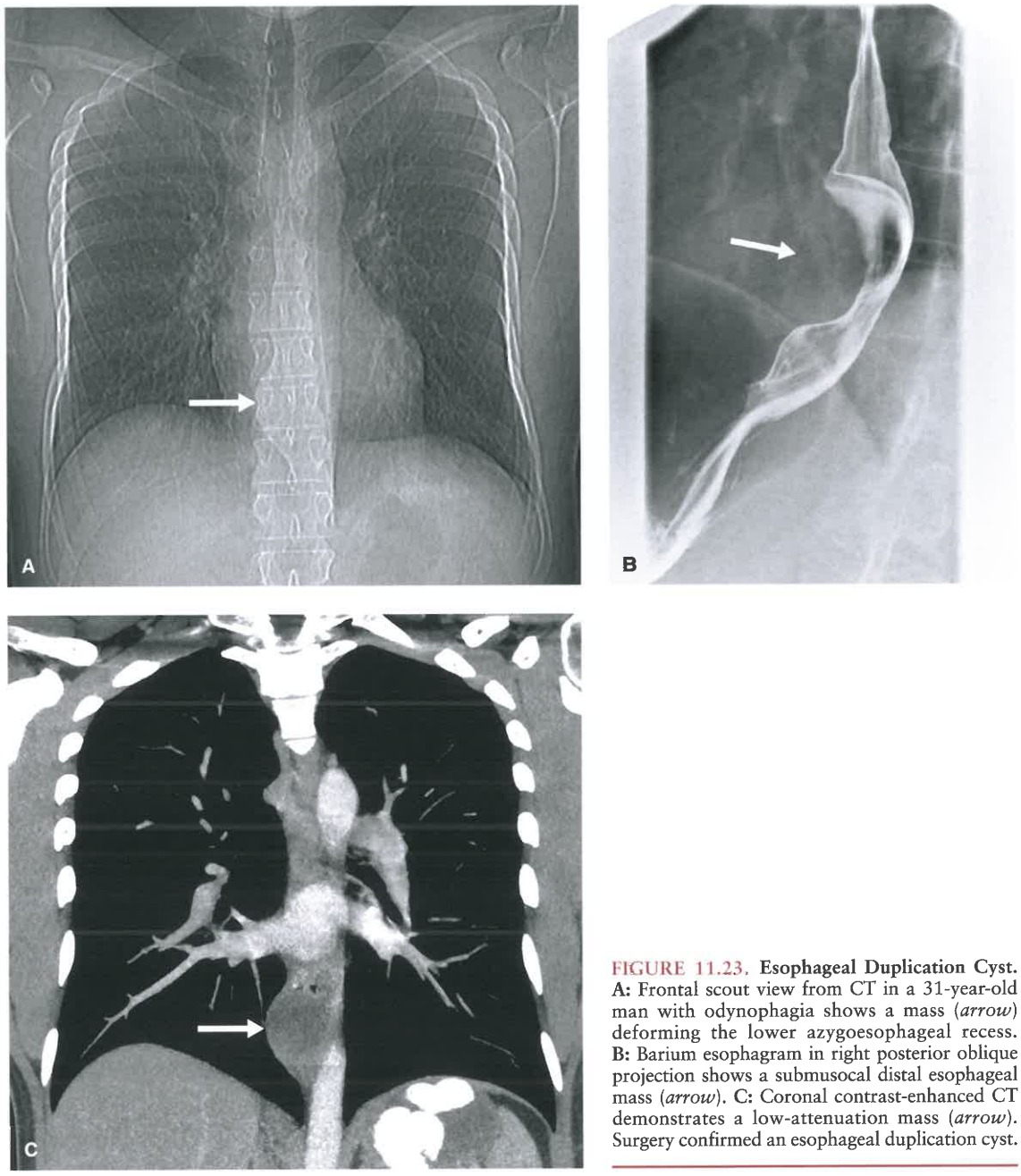

FIGURE 11.23. **Esophageal Duplication Cyst.** **A:** Frontal scout view from CT in a 31-year-old man with odynophagia shows a mass (*arrow*) deforming the lower azygoesophageal recess. **B:** Barium esophagram in right posterior oblique projection shows a submusocal distal esophageal mass (*arrow*). **C:** Coronal contrast-enhanced CT demonstrates a low-attenuation mass (*arrow*). Surgery confirmed an esophageal duplication cyst.

bone cyst); (2) extraosseous extension of infection, tumor, or marrow elements (infectious spondylitis (Fig. 11.26), metastatic carcinoma, extramedullary hematopoiesis, respectively); (3) pathologic fracture and paraspinal hematoma formation (any destructive neoplastic or inflammatory process, trauma); or (4) protrusion of degenerative osteophytes. Neoplastic processes are usually easily identified by expansion and destruction of vertebral bodies, with sparing of intervertebral disks. Bronchogenic, breast, or renal cell carcinoma are the most common primary sites of thoracic spinal metastases. Infectious spondylitis is distinguished from neoplastic processes by the presence of a paravertebral mass centered at the point of maximal bone destruction. In patients with a paravertebral abscess secondary to tuberculosis or bacterial infection, narrowing of the adjacent disk space and destruction of vertebral end-plates are important clues to the diagnosis. Extramedullary hematopoiesis is seen almost exclusively in conditions associated with ineffective production or excessive destruction of erythrocytes, such as thalassemia major, congenital spherocytosis, and sickle cell anemia. It is recognized by noting expansion of the medullary space and cyst formation within long bones, ribs, and vertebral bodies, with associated lobulated paraspinal soft tissue masses. These masses, which represent hyperplastic bone marrow that has extruded from the vertebral bodies and posterior ribs, are typically seen in the lower thoracic and upper lumbar region. Traumatic injuries to the thoracic spine are usually obvious from the patient's history and recognition of spine fracture on radiographic and CT studies of the spine. Degenerative disk disease may produce a localized paraspinal mass on frontal radiographs. Well-penetrated films will show the characteristic inferolaterally projecting osteophytes at the level of the mass, which are most commonly right sided because of the inhibitory

TABLE 11.5

POSTERIOR (PARAVERTEBRAL) MEDIASTINAL MASSES

Neurogenic	■ Intercostal nerve • Schwannoma • Neurofibroma • Neurofibrosarcoma ■ Sympathetic ganglia • Ganglioneuroma • Ganglioneuroblastoma • Neuroblastoma ■ Paraganglioma
Vertebral	■ Trauma • Paraspinal hematoma ■ Infection • Paraspinal abscess ■ Staphylococcus ■ Tuberculosis ■ Neoplasm • Metastatic disease • Myeloma • Lymphoma ■ Degenerative • Osteophytosis ■ Other • Extramedullary hematopoiesis
Vascular	■ Thoracic aortic aneurysm ■ Double aortic arch ■ Dilated azygos vein ■ Dilated main pulmonary artery ■ Esophageal varices
Cyst	■ Lateral thoracic meningocele

effect of the pulsating descending aorta on left-sided osteophyte formation.

Lateral Thoracic Meningoceles represent an anomalous herniation of the spinal meninges through an intervertebral foramen, resulting in a paravertebral soft tissue mass. Most meningoceles are discovered in middle-aged patients as asymptomatic masses. They are slightly more common on the right, and are multiple in 10% of cases. There is a high association between lateral thoracic meningoceles and neurofibromatosis. A meningocele is the most common posterior mediastinal mass in patients with neurofibromatosis; conversely, approximately two-thirds of patients with meningoceles have neurofibromatosis. Chest radiographs typically reveal a round, well-defined paraspinal mass that is indistinguishable from a neurofibroma. Additional clues to the diagnosis include rib erosion, enlargement of the adjacent neural foramen, vertebral anomalies, or kyphoscoliosis. When a lateral meningocele is associated with kyphoscoliosis, it is usually found at the apex of the scoliotic curve on the convex side. MR demonstration of a herniated subarachnoid space is the diagnostic technique of choice; conventional or CT myelography, which demonstrates filling of the meningocele with contrast, is reserved for equivocal cases.

Rarely, malignant lymph node enlargement may produce a recognizable paraspinal mass. This is most often seen in NHL, metastatic lung cancer, and seminoma; other mediastinal or extrathoracic sites of involvement are invariably present.

Despite the advances in detection and characterization of mediastinal masses with cross-sectional imaging, most patients will require tissue sampling for definitive diagnosis. However, the radiologist can use the information provided by CT or MR to help limit the differential diagnosis and thereby guide the appropriate evaluation and treatment. In a large percentage of cases, when tissue sampling is required, it can be accomplished by CT- or US-guided transthoracic biopsy.

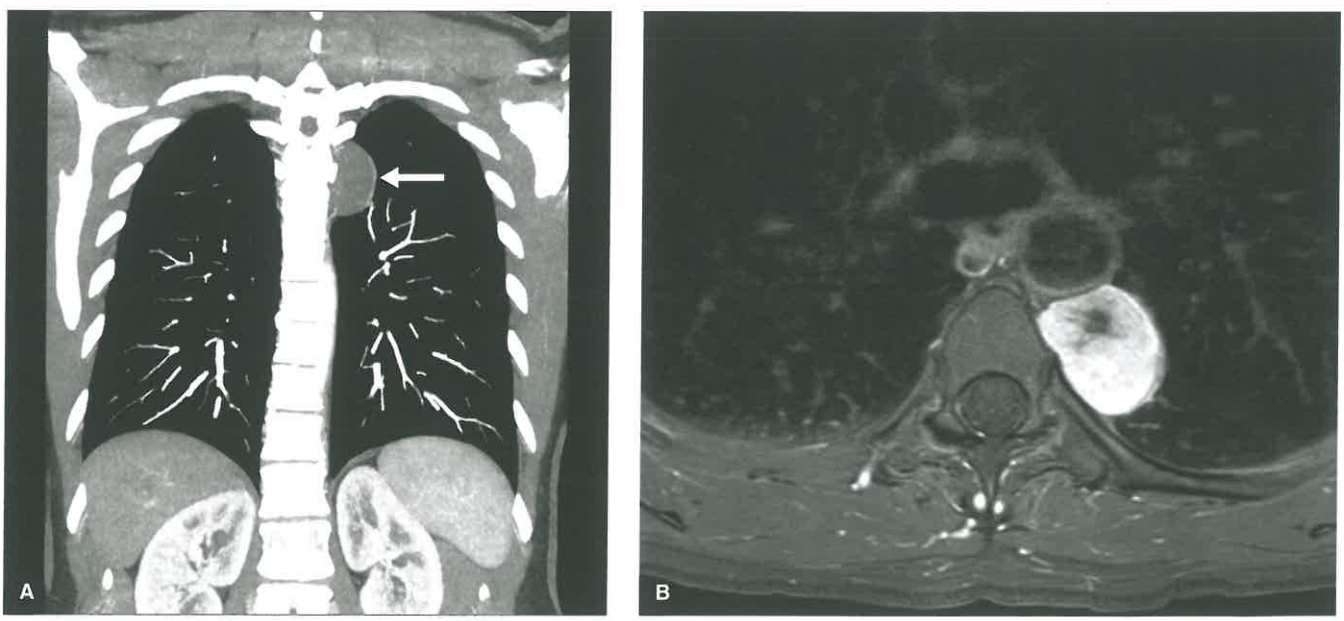

FIGURE 11.24. **Schwannoma. A:** Contrast-enhanced coronal maximum intensity projection CT in an asymptomatic 39-year-old woman demonstrates a left upper paravertebral soft tissue mass (*arrow*). **B:** Axial T1-weighted fat saturated post contrast MR shows enhancement of the lesion. CT-guided biopsy confirmed a schwannoma.

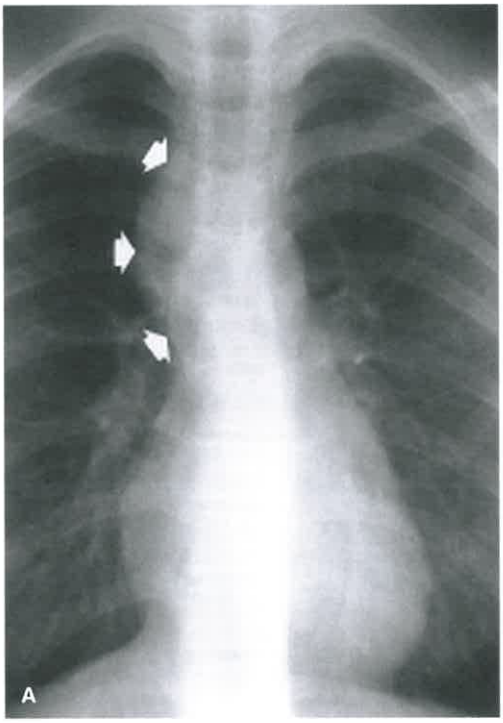

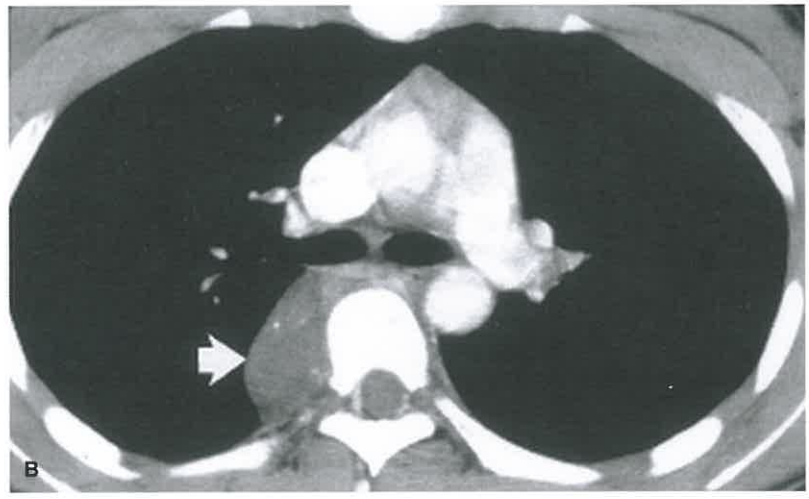

FIGURE 11.25. **Ganglioneuroma. A:** Posteroanterior radiograph in a 15-year-old female reveals an oval, vertically oriented, right-sided mediastinal mass (*arrows*). **B:** Contrast-enhanced CT shows a low-attenuation posterior mediastinal mass (*arrow*) with calcification. This was surgically proven to be ganglioneuroma.

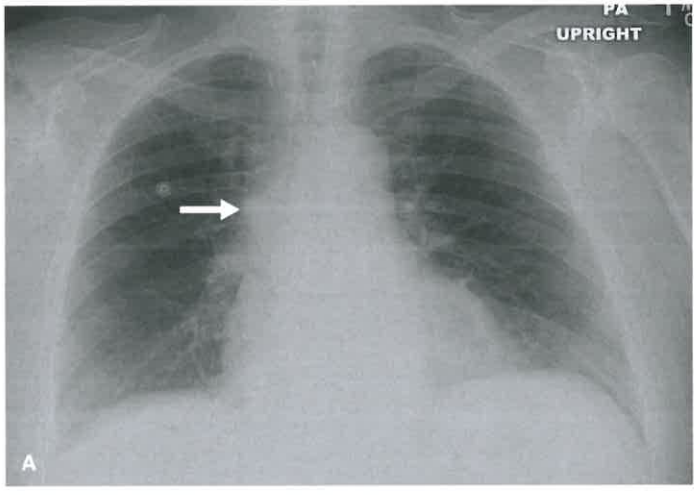

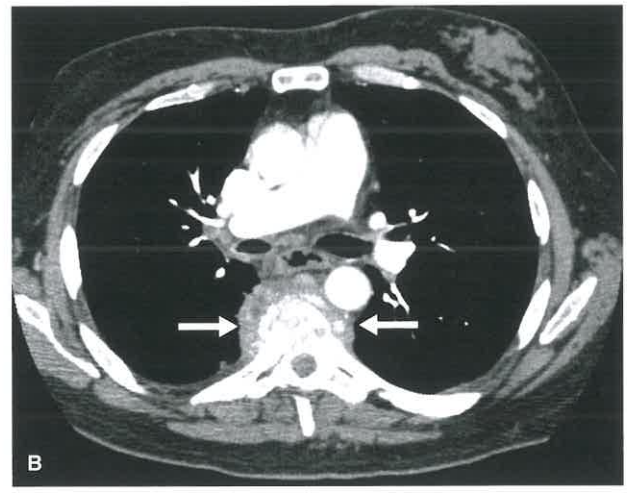

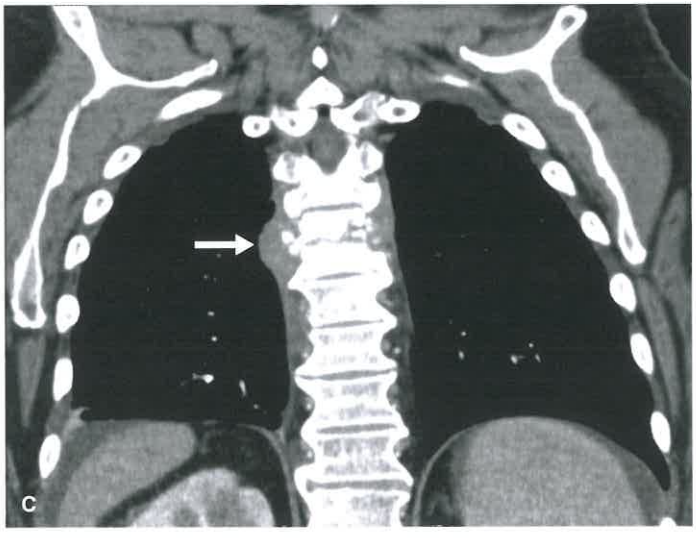

FIGURE 11.26. **Discitis/Osteomyelitis of Thoracic Spine as Paravertebral Mass. A:** Frontal chest radiograph in a 53-year-old man with cirrhosis, fever, and back pain shows a subtle right mediastinal mass (*arrow*). **B, C:** Axial (B) and coronal (C) contrast-enhanced CT shows disc space narrowing and vertebral end-plate destruction with a paravertebral inflammatory mass (*arrows*). Biopsy showed staphylococcal infection.

DIFFUSE MEDIASTINAL DISEASE (TABLE 11.6)

Mediastinal Infection is an uncommon condition that may be divided into acute and chronic forms based upon etiology, clinical features, and radiologic findings. The distinction between acute and chronic infection is important because there are considerable differences in treatment and prognosis.

Acute mediastinitis is caused by bacterial infection that most often develops following esophageal perforation or is a complication of cardiothoracic or esophageal surgery. Esophageal perforation may complicate esophageal instrumentation (e.g., endoscopy, biopsy, dilatation, or stent placement); penetrating chest trauma; esophageal carcinoma; foreign body or corrosive ingestion; or vomiting. Spontaneous esophageal perforation following prolonged vomiting is termed *Boerhaave syndrome*. In this condition, a vertical tear occurs along the left posterolateral wall of the distal esophagus, just above the esophagogastric junction, leading to signs and symptoms of acute mediastinitis. Less commonly, acute mediastinitis may develop from mediastinal extension of infection in the neck, retropharyngeal space, lungs, pleural space, pericardium, or spine.

The clinical presentation of acute mediastinitis is usually dramatic and is characterized by severe retrosternal chest pain, fever, chills, and dysphagia, often accompanied by evidence of septic shock. Physical examination may reveal findings associated with pneumomediastinum, with subcutaneous emphysema in the neck and an apical, systolic crunching sound on chest auscultation (Hamman sign).

The most common chest radiographic findings are widening of the superior mediastinum in 66% of patients and pleural effusion in 50% of patients. Specific findings such as mediastinal air or air–fluid levels are less common. When mediastinitis occurs in association with Boerhaave syndrome, pneumoperitoneum and left hydropneumothorax may also be seen.

When esophageal perforation is suspected, an esophagram or CT with oral contrast should be performed to detect leakage of contrast into the mediastinum and to localize the exact site of perforation. In a patient who is not at risk for aspiration, a water-soluble contrast agent is administered initially. Once gross contrast extravasation has been excluded, barium is then given for superior radiographic detail. The sensitivity of the esophagram for detecting contrast leakage is highest when the study is obtained within 24 hours of the perforation.

MDCT is the radiologic study of choice for the diagnosis of acute mediastinitis. CT findings include extraluminal gas, bulging of the mediastinal contours, and focal or diffuse soft tissue infiltration of mediastinal fat. Localized fluid collections suggest focal abscess formation (Fig. 11.27). Associated findings include mediastinal venous thrombosis, pneumothorax, pleural effusion or empyema, subphrenic abscess, and vertebral osteomyelitis.

While the clinical and radiographic diagnosis of mediastinitis is often straightforward, it may be difficult in postoperative patients who have undergone recent median sternotomy. In these patients, infiltration of mediastinal fat and focal air or fluid collections may be normal findings on postoperative CT scans performed days to weeks following the removal of intraoperatively placed mediastinal drains. In such patients, the progression of findings on follow-up CT scans will correctly identify the majority of those with postoperative mediastinal infection.

The prognosis for patients with acute mediastinitis varies with the underlying etiology and the extent of mediastinal involvement at the time of diagnosis. Esophageal perforation is associated with the poorest outcome, with a mortality approaching 50%. A delay in diagnosis and treatment of the mediastinal infection of greater than 24 hours is associated with a significant increase in overall morbidity and mortality.

In addition to its sensitivity in the diagnosis of mediastinitis, CT can be used to guide treatment and predict outcome. Those patients with evidence of extensive mediastinal infection, seen on CT as diffuse infiltration of the mediastinal fat without evidence of abscess formation, have a mortality approaching 50%. In contrast, patients with discrete mediastinal abscesses that are amenable to surgical or percutaneous drainage, or with small localized abscesses that are amenable to antibiotic therapy alone, have a more favorable prognosis. In addition, patients with mediastinal abscesses and contiguous empyema or subphrenic abscess may respond favorably to drainage of these extramediastinal collections.

Chronic Fibrosing (Sclerosing) Mediastinitis. The hallmarks of chronic fibrosing mediastinitis are chronic inflammatory changes and mediastinal fibrosis. The most common cause of this rare condition is granulomatous infection, usually secondary to *Histoplasma capsulatum*. Infection by other fungi including blastomycosis and aspergillosis, tuberculosis, radiation therapy, sarcoidosis and drugs (methysergide) are less common causes. Idiopathic mediastinal fibrosis, which is probably an autoimmune process, is related to fibrosis in other regions, including the retroperitoneum, intraorbital fat, and thyroid gland.

Several theories have been advanced to explain the pathogenesis of fibrosing mediastinitis owing to histoplasmosis. The most widely accepted theory suggests that affected patients develop an idiosyncratic hypersensitivity response to a fungal antigen released from ruptured mediastinal granulomas resulting in a fibroinflammatory reaction.

TABLE 11.6

DIFFUSE MEDIASTINAL WIDENING

Smooth	■ Mediastinal lipomatosis ■ Malignancy • Lymphoma • Small cell carcinoma • Metastatic disease ■ Mediastinal hemorrhage • Arterial • Traumatic aortic/arch vessel laceration • Ruptured aortic aneurysm • Venous • Superior vena cava/right atrial injury ■ Mediastinitis • Acute bacterial • Chronic (sclerosing) • Histoplasmosis • Other ■ Dilated esophagus • Achalasia • Scleroderma • Stricture • Distal esophageal malignancy
Lobulated	■ Lymph node enlargement (see Table 11.3) ■ Malignancy • Small cell carcinoma • Metastatic disease ■ Vascular • Tortuous great vessels ■ Superior vena cava thrombosis ■ Neurofibromatosis

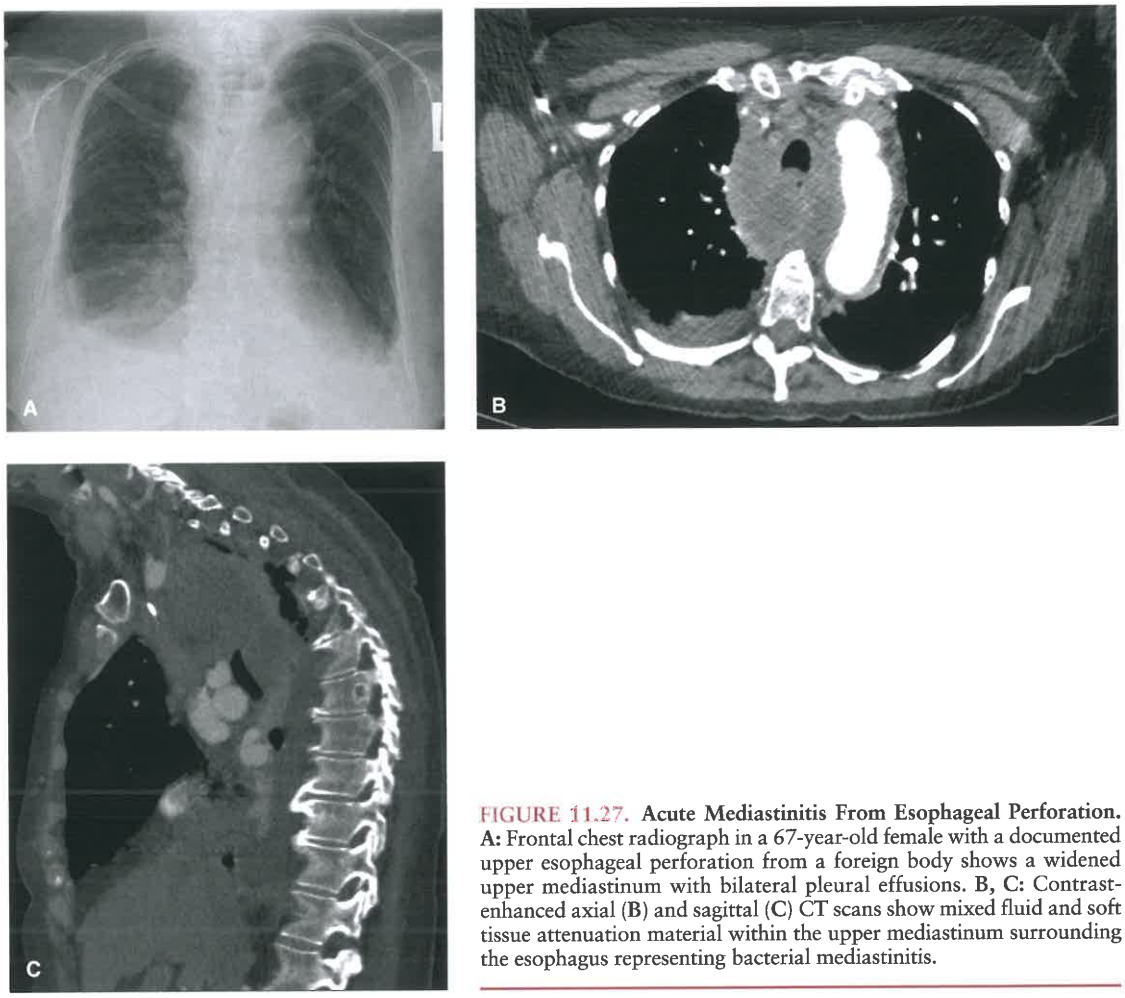

FIGURE 11.27. **Acute Mediastinitis From Esophageal Perforation.** **A:** Frontal chest radiograph in a 67-year-old female with a documented upper esophageal perforation from a foreign body shows a widened upper mediastinum with bilateral pleural effusions. **B, C:** Contrast-enhanced axial (**B**) and sagittal (**C**) CT scans show mixed fluid and soft tissue attenuation material within the upper mediastinum surrounding the esophagus representing bacterial mediastinitis.

Clinically, this condition occurs in adults and presents with a variety of symptoms, depending upon the extent of fibrosis and the mediastinal structures compromised by the fibrotic process. The superior vena cava (SVC) is the most commonly affected structure, with involvement in over 75% of symptomatic patients. The SVC syndrome manifests with headache, epistaxis, cyanosis, jugular venous distention, and edema of the face, neck, and upper extremities. The most serious and potentially fatal manifestation of fibrosing mediastinitis is obstruction of the central pulmonary veins, which produces pulmonary edema that may mimic severe mitral stenosis. Patients with involvement of the tracheobronchial tree may have cough, dyspnea, wheezing, hemoptysis, and obstructive pneumonitis. Dysphagia or hematemesis can be seen with esophageal involvement. Less commonly, pulmonary arterial hypertension and cor pulmonale can develop from narrowing of the pulmonary arteries. Rarely constrictive pericarditis can develop.

The most common finding noted on chest radiographs is asymmetric lobulated widening of the upper mediastinum, most often on the right. When the process is secondary to granulomatous infection, enlarged calcified lymph nodes may be seen. Narrowing of the tracheobronchial tree may be evident. The sequelae of vascular involvement may be seen, including oligemia from pulmonary arterial compression or venous hypertension and pulmonary edema from involvement of the central pulmonary veins. Postobstructive atelectasis or consolidation may also be seen.

MDCT is the modality of choice for the diagnosis and assessment of chronic sclerosing mediastinitis. Enlarged lymph nodes with calcification are the most common finding (Fig. 11.28). The fibrotic infiltration of the mediastinal fat that is characteristic of this condition is seen as abnormal soft tissue density replacing the normal mediastinal fat with obliteration of the normal mediastinal interfaces. MDCT delineates the degree of involvement of the mediastinal vessels, trachea, and central bronchi. In patients with significant SVC involvement, collateral venous channels within the mediastinum and chest wall are well demonstrated.

A definitive diagnosis of chronic fibrosing mediastinitis and the establishment of the underlying etiology are difficult. Skin tests for histoplasmosis and tuberculosis may add additional information but are usually not helpful. The precise diagnosis, and more important the distinction from infiltrating malignancy, may require biopsy, but in most cases typical imaging findings provide a confident presumptive diagnosis. In those patients with noncalcified mediastinal or hilar masses that lack ancillary findings of histoplasmosis such as lung, hepatic, or splenic calcifications, biopsy may be necessary to establish a diagnosis.

Mediastinal Hemorrhage. Injury to mediastinal vessels resulting from blunt or penetrating thoracic trauma is the most common cause of mediastinal hemorrhage. Blunt chest trauma most often occurs in the setting of a motor vehicle accident, when rapid deceleration and thoracic cage compression produce shearing effects at the aortic isthmus. Iatrogenic trauma, usually from attempts at central line placement, can also cause mediastinal hemorrhage. Spontaneous hemorrhage

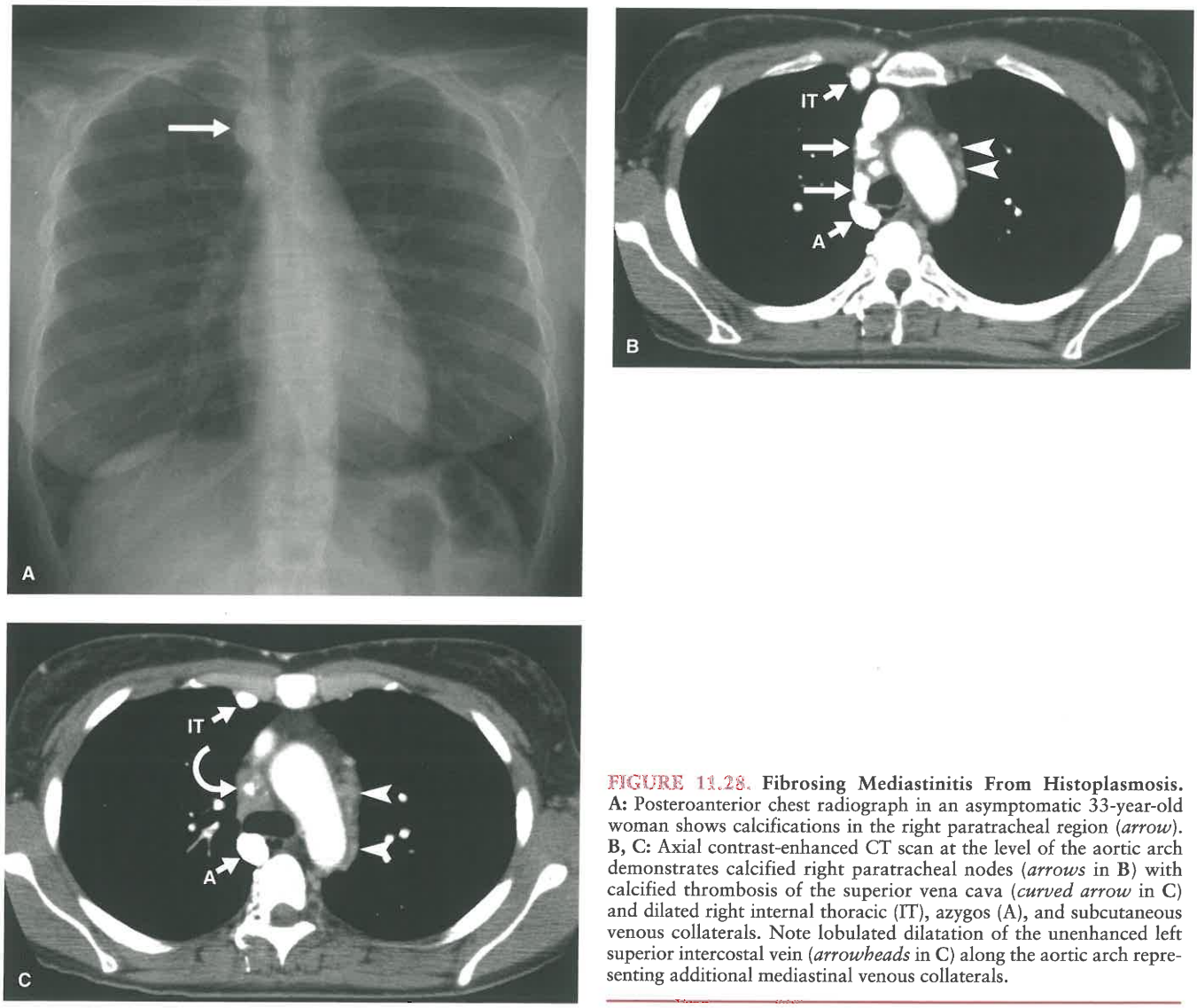

FIGURE 11.28. **Fibrosing Mediastinitis From Histoplasmosis.** **A:** Posteroanterior chest radiograph in an asymptomatic 33-year-old woman shows calcifications in the right paratracheal region (*arrow*). **B, C:** Axial contrast-enhanced CT scan at the level of the aortic arch demonstrates calcified right paratracheal nodes (*arrows* in **B**) with calcified thrombosis of the superior vena cava (*curved arrow* in **C**) and dilated right internal thoracic (IT), azygos (A), and subcutaneous venous collaterals. Note lobulated dilatation of the unenhanced left superior intercostal vein (*arrowheads* in **C**) along the aortic arch representing additional mediastinal venous collaterals.

may develop in patients with a coagulopathy, or with aortic rupture from aneurysm or dissection. Chronic hemodialysis, radiation vasculitis, and bleeding into a mediastinal mass are rare causes of mediastinal hemorrhage.

In the nontraumatic setting, the signs and symptoms of mediastinal hemorrhage are often mild or absent. The patient may complain of retrosternal chest pain radiating toward the back. Rarely, SVC compression may result in the SVC syndrome. Extension of blood from the mediastinum superiorly into the retropharyngeal space may result in neck stiffness, odynophagia, or stridor.

The main radiographic finding in mediastinal hemorrhage of any cause is a focal or diffuse widening of the mediastinum that obscures the normal mediastinal contours. In mediastinal hemorrhage, the mediastinum develops a flat or slightly convex outward contour, unlike the round, lobulated, or irregular contour seen with enlarged lymph nodes or a localized mediastinal mass. Blood extending from the mediastinum into the pleural or extrapleural space produces a free-flowing effusion or a loculated extrapleural collection, respectively. Rarely, extension of blood into the lungs via the bronchovascular interstitium produces interstitial opacities that mimic pulmonary edema. Serial radiographs may show rapid changes in mediastinal or pleural fluid collections in patients with persistent hemorrhage. CT demonstrates abnormal soft tissue within the mediastinum that obliterates the normal interfaces between the mediastinal fat, the vessels, and the airways (Fig. 11.29). Freshly clotted blood is high in attenuation and is usually easily appreciated on CT. CT is also superior to radiography in demonstrating the extramediastinal extent of hemorrhage and is useful in demonstrating associated thoracic injuries in patients following blunt chest trauma.

Mediastinal Lipomatosis is a benign, asymptomatic condition characterized by excessive deposition of fat in the mediastinum. Predisposing conditions include obesity, Cushing disease, and corticosteroid therapy. However, this entity is unassociated with identifiable conditions in approximately 50% of patients.

The common finding on conventional radiography is smooth, symmetric widening of the superior mediastinum. If the amount of fat deposition is marked, the mediastinum widening may show lobulated margins. The trachea remains midline in position in patients with mediastinal lipomatosis, whereas mediastinal tumor infiltration or mediastinal hemorrhage usually cause tracheal deviation or narrowing. Fat may also accumulate in the paraspinal regions, chest wall, and cardiophrenic angles; the latter produces enlargement of the epipericardial fat pads that is a clue to the proper diagnosis.

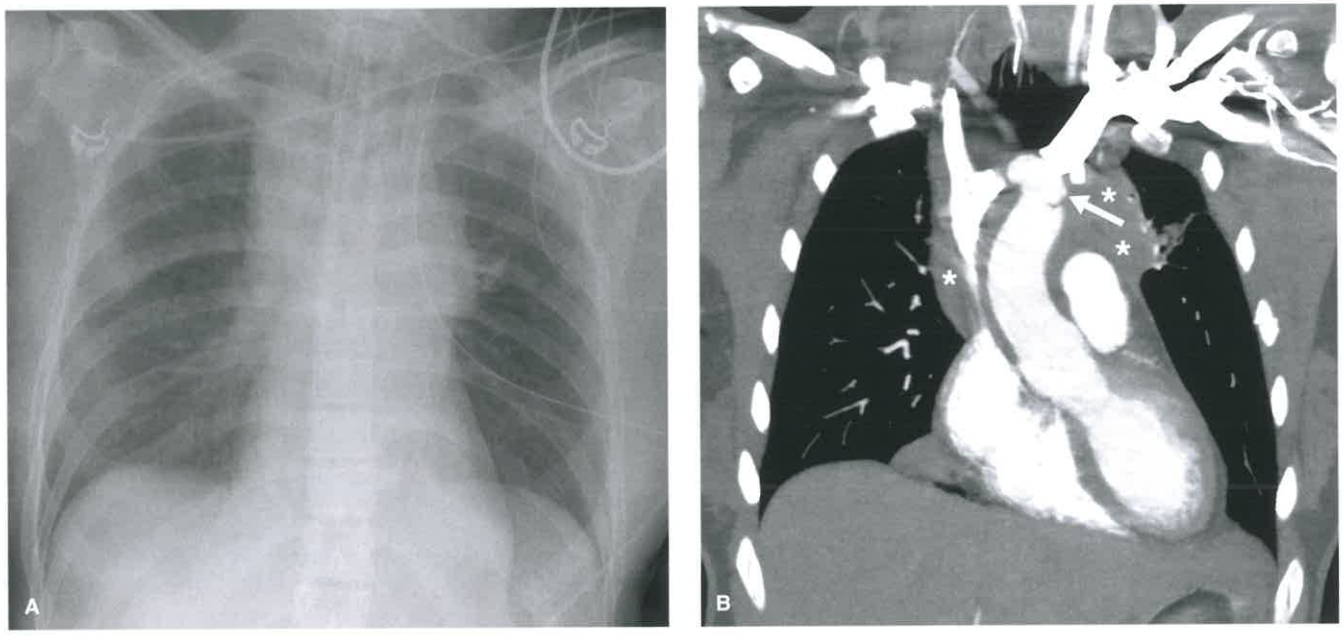

FIGURE 11.29. **Mediastinal Hematoma From Traumatic Aortic Injury. A:** Portable chest radiograph in a 38-year-old woman involved in a motor vehicle accident demonstrates a widened mediastinum. **B:** Coronal maximum intensity projection CT aortogram demonstrates a traumatic pseudoaneurysm of the aortic arch (*arrow*) with extensive mediastinal hematoma (*asterisks*).

CT provides a definitive diagnosis by demonstrating abundant, homogeneous, unencapsulated fat that bulges the mediastinal contours (Fig. 11.30). Displacement or compression of mediastinal structures, particularly the trachea, is typically absent. Heterogeneity within the fat suggests other primary or superimposed conditions, such as neoplastic infiltration, infection, hemorrhage, or fibrosis.

Malignancy. Malignant involvement of the mediastinum is typically seen as discrete masses or lymph node enlargement. Rarely, diffuse soft tissue infiltration of the mediastinal fat may occur, either alone or in association with focal lesions. Plain radiographs are nonspecific, usually demonstrating mediastinal widening. CT shows soft tissue infiltration of the normal mediastinal fat and obliteration of the normal tissue planes. This pattern is most common with extracapsular spread of lymphoma or small cell carcinoma of the lung. The latter disease has a high propensity to invade mediastinal structures and therefore may present with symptoms of airway obstruction or SVC syndrome.

Pneumomediastinum is the presence of extraluminal gas within the mediastinum. Possible sources of such gas include the lungs, trachea, central bronchi, esophagus, external trauma including surgery and penetrating injury, and extension of gas from the neck or abdomen (Table 11.7).

Air from the lungs is the most common source of pneumomediastinum. The mechanism of pneumomediastinum formation involves a sudden rise in intrathoracic and intra-alveolar pressure that leads to alveolar rupture. The extra-alveolar air first collects within the bronchovascular interstitium and then dissects centrally to the hilum and mediastinum (the Macklin

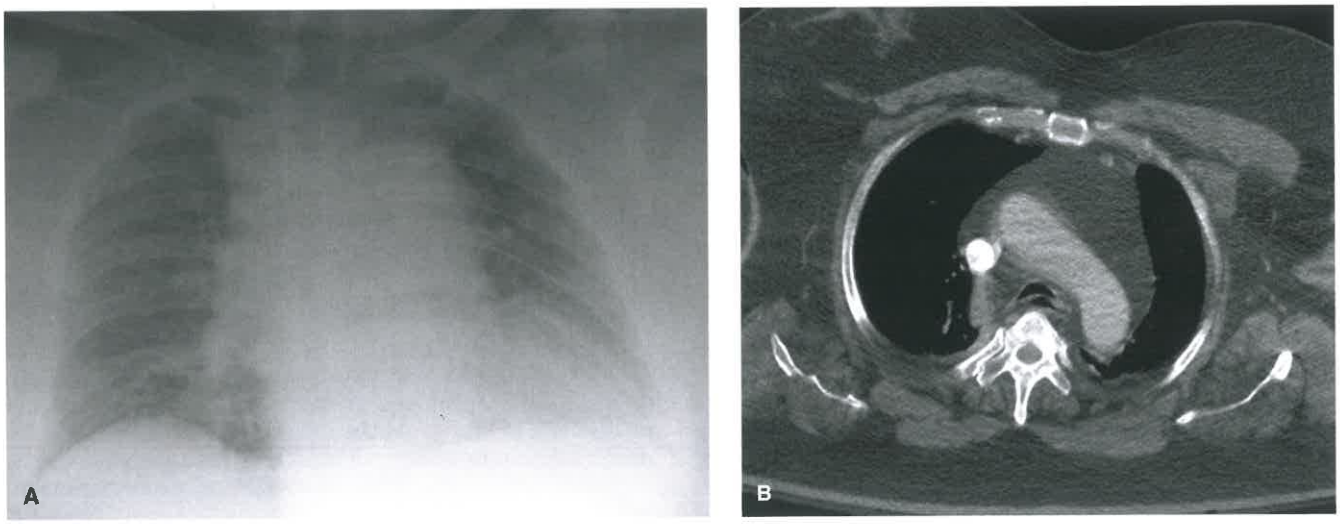

FIGURE 11.30. **Mediastinal Lipomatosis. A:** Frontal chest radiograph in a 54-year-old man shows a widened mediastinum. **B:** Axial contrast-enhanced CT at the level of the aortic arch shows abundant mediastinal fat accounting for the mediastinal widening on radiography.

TABLE 11.7

CAUSES OF PNEUMOMEDIASTINUM

Intrathoracic	■ Alveolar • Valsalva maneuver • Positive pressure ventilation ■ Tracheobronchial tree • Bronchial stump dehiscence • Tracheobronchial injury ■ Esophagus • Boerhaave syndrome • Traumatic esophageal injury ■ Endoscopic interventions • Carcinoma with fistula ■ Infection with fistula formation • Histoplasmosis • Tuberculosis
Extrathoracic	■ Recent sternotomy ■ Pneumoperitoneum/ pneumoretroperitoneum ■ Subcutaneous emphysema in neck ■ Penetrating injury ■ Laryngeal injury

effect). Less commonly, the air may dissect peripherally toward the subpleural interstitium and rupture through the visceral pleura to produce a pneumothorax.

Pneumomediastinum most commonly complicates mechanical ventilation in patients with ARDS, because the combination of positive pressure ventilation and noncompliant lungs predisposes to alveolar rupture. Spontaneous pneumomediastinum can occur with deep inspiratory or Valsalva maneuvers during strenuous exercise, childbirth, weightlifting, and inhalation of drugs such as marijuana, nitrous oxide, and crack cocaine. Patients with asthma are prone to pneumomediastinum; this is related to the airways obstruction that characterizes this disease (Fig. 11.31). Prolonged vomiting from any cause may lead to intrathoracic pressures that are sufficiently high to produce pneumomediastinum. In patients with diabetic ketoacidosis, pneumomediastinum may result from the deep inspirations associated with Kussmaul breathing as patients attempt to correct the underlying acidosis. Blunt chest trauma can result in pneumomediastinum as a result of an abrupt increase in intra-alveolar pressure and shearing forces affecting the alveolar walls.

Pneumomediastinum arising from the tracheobronchial tree or esophagus usually is a result of traumatic disruption of these structures. The marked shearing forces that develop with blunt trauma may lead to fracture of the trachea or mainstem bronchi. Penetrating trauma to the tracheobronchial tree is usually iatrogenic and may follow endotracheal intubation, bronchoscopy, or tracheostomy. Rarely, neoplasms or inflammatory lesions (e.g., tuberculosis) may erode through the tracheal wall and into the peritracheal fat. Esophageal rupture is most often spontaneous, usually in the setting of severe, prolonged vomiting (Boerhaave syndrome). In addition to pneumomediastinum, a left hydropneumothorax and pneumoperitoneum may be present in this condition. Spontaneous esophageal rupture may occur during childbirth, during a severe asthmatic episode, or with blunt chest trauma. Endoscopic procedures, stent placement, esophageal dilatation, corrosive ingestion, and carcinoma may lead to esophageal perforation. Mediastinal gas may be produced by bacterial organisms in acute mediastinitis.

Air within the soft tissues of the neck from penetrating trauma or laryngeal fracture may lead to pneumomediastinum by extending inferiorly through the retropharyngeal and prevertebral spaces, or along the sheaths of the great vessels. Deep space infections in the neck can spread along the same fascial planes and lead to mediastinitis. The term *Ludwig angina* describes the substernal chest pain caused by the intramediastinal extension of such infections. Rarely, pneumomediastinum develops as air dissects superiorly from the retroperitoneum through the aortic hiatus or from the peritoneal cavity along the internal mammary vascular sheaths.

The symptoms associated with pneumomediastinum vary with the underlying etiology, extent of mediastinal air, and presence of mediastinitis. Mediastinal air without infection is generally asymptomatic and does not require treatment. In some patients with spontaneous pneumomediastinum, there may be substernal, pleuritic-type chest pain of sudden onset that can be related to a specific inciting incident, such as vomiting or the Valsalva maneuver. Dyspnea may be present. In adults, mediastinal air under pressure usually escapes into the neck, producing crepitus over the neck, supraclavicular regions, and chest wall. Rarely, mediastinal air under pressure may produce a tension pneumomediastinum in which the clinical findings are those of cardiac tamponade. Patients with mediastinitis and pneumomediastinum are usually seriously ill with chest pain, high fevers, dyspnea, and signs of sepsis. The radiographic findings of pneumomediastinum are reviewed in Chapter 10.

THE HILA

Unilateral Hilar Enlargement/Increased Density (Table 11.8)

An abnormal hilum as seen radiographically can appear as enlargement, increased density, or both. Increased density can occasionally result from a parenchymal abnormality superimposed on the hilum on frontal radiography, and while the lateral radiograph is most helpful in this regard, CT will often be necessary to localize the abnormality to the hilum. Comparison with the contralateral hilum and review of prior radiographs are most helpful in detecting hilar abnormality.

Malignancy. A hilar mass usually represents bronchogenic carcinoma or confluent lymph node metastases (Fig. 11.32). Unilateral hilar enlargement may be the presenting radiographic feature of squamous cell carcinoma, where the hilar mass represents the extraluminal extension of an endobronchial tumor from its origin within a central (i.e., lobar or proximal segmental) bronchus. Concomitant hilar lymph node involvement may contribute to hilar enlargement in some of these patients. Approximately 20% of patients with squamous cell carcinoma have a hilar mass on chest radiograph. In contrast, patients with adenocarcinoma and large cell carcinoma more commonly present with a peripheral pulmonary nodule or mass. In many patients, the hilar mass may be obscured by adjacent atelectasis or obstructive pneumonitis.

Unilateral hilar enlargement resulting from metastatic lymph node involvement is most often seen in small cell carcinoma (Fig. 11.15). The propensity of this tumor for early invasion of the bronchial submucosa and peribronchial lymphatics accounts for the high incidence of widespread hematogenous and hilar and mediastinal lymph node metastases at the time of diagnosis. Plain film evidence of enlarged hilar lymph nodes resulting from metastases from adenocarcinoma of lung or large cell carcinoma are seen in only 10% to 15% of patients. CT is more sensitive than radiography for detecting enlarged hilar nodes and should be performed in all patients to guide further staging procedures and for proper preoperative or treatment planning.

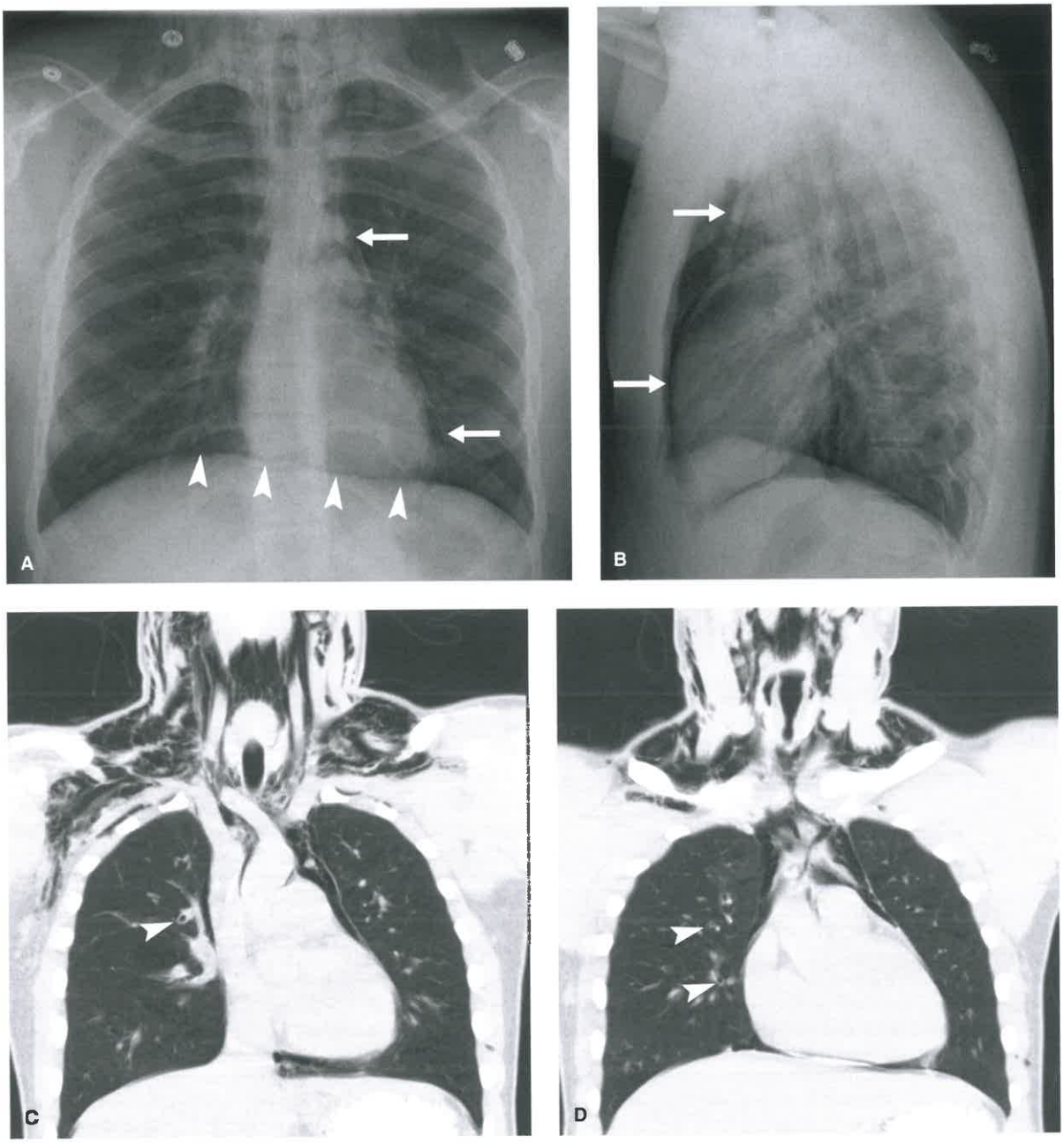

FIGURE 11.31. **Pneumomediastinum. A, B:** Frontal (**A**) and lateral (**B**) chest radiographs in a patient with an acute asthma exacerbation shows perihilar bronchial cuffing (*arrow*) and pneumomediastinum extending into the neck producing subcutaneous emphysema. Note the ability to see the diaphragm as a continuous interface ("continuous diaphragm" sign) (*arrowheads*). **C, D:** Coronal CT scans at the level of the ascending aorta show airways thickening (*arrow*) and confirms pneumomediastinum extending into the neck.

Metastases to hilar and mediastinal lymph nodes from extrathoracic malignancies are uncommon, occurring in approximately 2% of patients. The malignancies that are most often associated with intrathoracic nodal metastases are genitourinary (renal and testicular); head and neck (skin, larynx, and thyroid); breast; and melanoma (Fig. 11.33). In renal cell carcinoma and seminoma, lymphatic spread of tumor to retroperitoneal nodes and up the thoracic duct to the posterior mediastinum is the mode of spread to thoracic nodes. Although there is no direct communication between the thoracic duct and anterior mediastinal lymph nodes, reflux of tumor emboli through incompetent valves may allow tumor spread to hilar, paratracheal, and intraparenchymal lymphatics. Head and neck tumors reach the mediastinum via lymphatic spread from cervical lymph nodes. Intrathoracic nodal metastases from breast carcinoma are often seen late in the course of disease, often years after the initial diagnosis. Malignant melanoma is the extrathoracic neoplasm with the highest incidence of intrathoracic nodal metastases; patients with nodal disease will almost invariably have radiographic evidence of parenchymal metastases.

Although 75% of patients presenting with Hodgkin lymphoma have evidence of intrathoracic lymph node enlargement, isolated unilateral hilar lymph node enlargement is uncommon. The thoracic manifestations in NHL differ in primary pulmonary lymphoma versus lymphoma that primarily

TABLE 11.8

UNILATERAL HILAR ENLARGEMENT

Lymph node enlargement	Malignancy	■ Bronchogenic carcinoma ■ Lymph node metastases • Bronchogenic carcinoma • Head and neck CA • Breast carcinoma • Melanoma • Genitourinary malignancy ■ Renal cell carcinoma ■ Testicular malignancy ■ Lymphoma
	Infection	■ Mycobacterial infection • TB • Nontuberculous (MAI) ■ Fungal infection • Histoplasmosis • Coccidioidomycosis • Blastomycosis ■ Bacterial • Lung abscess • Plague • Tularemia ■ Viral infection • Measles • Mononucleosis
Vascular	Pulmonary artery dilation	■ Valvular pulmonic stenosis (left) ■ Pulmonary artery aneurysm • Behçet's • Hughes–Stovin ■ Pulmonary artery thromboembolism
Cyst	Foregut	Bronchogenic cyst

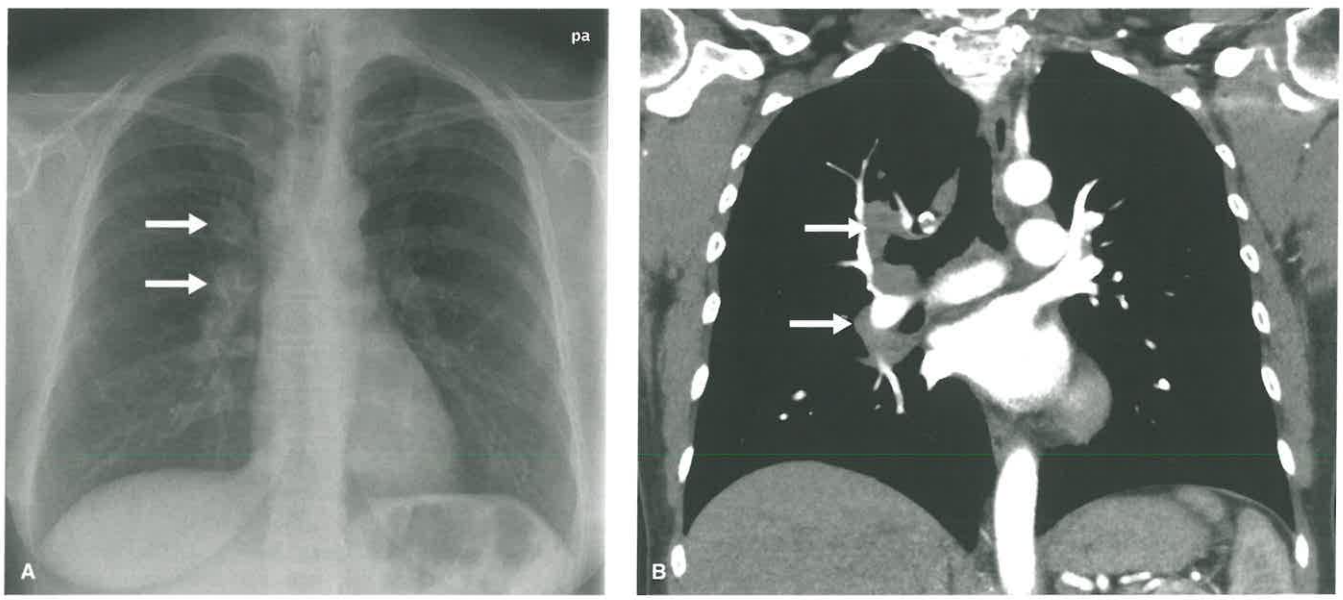

FIGURE 11.32. **Bronchogenic Carcinoma as Enlarged Hilar Lymph Nodes. A:** Frontal chest radiograph in a 49-year-old woman with chest tightness shows an enlarged right hilum (*arrows*). **B:** Coronal contrast-enhanced CT through the right hilum shows a enlarged right hilar lymph nodes (*arrows*). Bronchoscopic biopsy revealed non–small cell carcinoma.

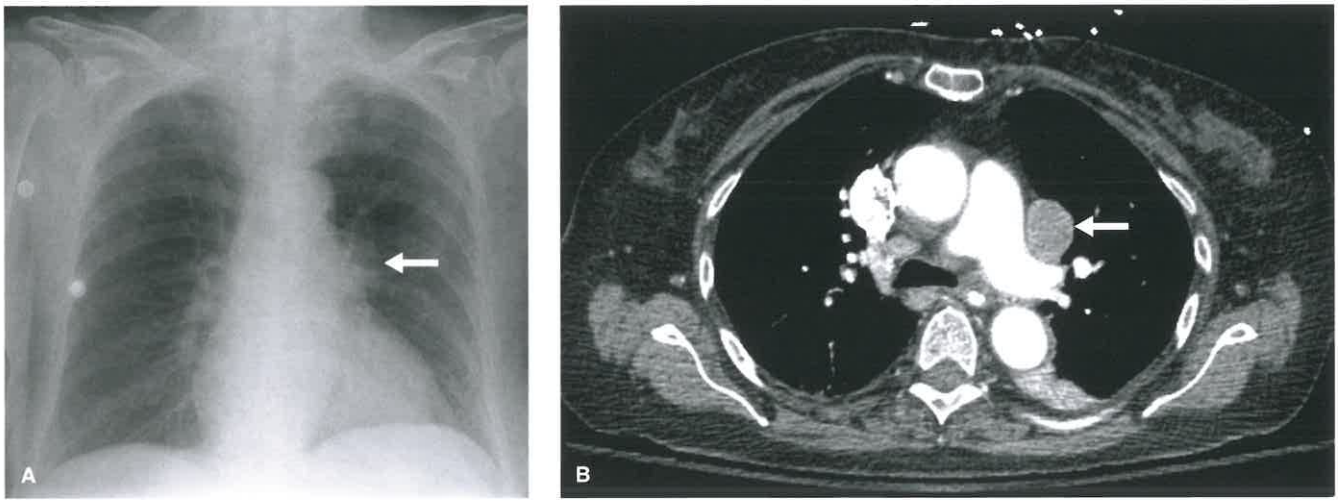

FIGURE 11.33. **Hilar Nodal Metastases From Ovarian Carcinoma. A:** Frontal chest radiograph in an 83-year-old woman with ovarian carcinoma shows a left hilar mass (*arrow*). **B:** Axial contrast-enhanced CT shows an enlarged left hilar lymph node (*arrow*) reflecting metastatic disease.

involves extrathoracic sites with secondary pulmonary involvement. Thoracic involvement in primary pulmonary lymphoma is largely limited to parenchymal and pleural disease, whereas secondary pulmonary lymphoma generally manifests as intrathoracic lymph node enlargement, with 35% showing hilar or middle mediastinal lymph node enlargement (Fig. 11.14).

Infection. Unilateral hilar or mediastinal lymph node enlargement is a characteristic feature in primary pulmonary tuberculosis (see Fig. 14.8) in distinction to postprimary tuberculosis; an exception is the severely immunocompromised patient with AIDS. Isolated lymph node enlargement as a manifestation of primary tuberculosis is more common in children than in adults. There is almost always concomitant parenchymal disease in immunocompetent patients with lymph node enlargement. Fungal infections such as histoplasmosis and coccidioidomycosis may present with hilar lymph node enlargement, typically associated with patchy or lobar airspace opacification in the ipsilateral lung (see Fig. 14.17). A variety of bacterial infections have been associated with unilateral hilar lymph node enlargement, including plague, tularemia, and anaerobic lung abscess. A characteristic finding in patients with pneumonic plague is the detection on unenhanced CT of increased attenuation within hilar and mediastinal nodes that drain regions of parenchymal involvement owing to intranodal hemorrhage. Tularemia (*Francisella tularensis*) causes parenchymal consolidation in association with hilar lymph node enlargement and pleural effusion.

The viral infections most commonly associated with hilar lymph node enlargement are infectious mononucleosis and measles pneumonia. The thorax is infrequently involved in mononucleosis, but hilar lymph node enlargement is the most common manifestation of intrathoracic disease. Lymph node enlargement may accompany the reticular interstitial opacities of typical measles pneumonia, or it may be associated with nodular, segmental, or lobar opacities and pleural effusion in atypical measles pneumonia.

Pulmonary Artery Enlargement. Although unilateral hilar enlargement is most often the result of a mass or enlarged lymph nodes, abnormal enlargement of the right or left pulmonary artery may cause hilar enlargement (Fig. 11.34). Vascular disorders that produce unilateral pulmonary artery enlargement include poststenotic dilatation of the left pulmonary artery from valvular or postvalvular pulmonic stenosis (Fig. 11.35), pulmonary artery aneurysms, and distention of the pulmonary artery by bland or tumor thrombus. Patients with congenital valvular pulmonic stenosis may develop poststenotic dilatation or aneurysms of the main and left pulmonary arteries from the jet effect of blood upon these vessels. Rarely, stenoses resulting from pulmonary artery vasculitis, congenital rubella, or Williams syndrome may lead to poststenotic dilatation of a pulmonary artery. Aneurysms of the central pulmonary arteries are usually associated with congenital heart disease, such as pulmonic stenosis and left-to-right shunts from ventricular septal defect and patent ductus arteriosus. Rare vasculitides such as Behçet disease and Hughes–Stovins syndrome may present with pulmonary artery aneurysms. A large pulmonary embolus lodging in the proximal portion of a pulmonary artery may cause proximal dilatation. Obviously, these patients are symptomatic and will show characteristic findings on perfusion lung scan or CT pulmonary angiography.

Bronchogenic Cyst is an uncommon cause of a hilar mass. CT and MR will show a round, smooth, thin-walled cyst, usually found in an asymptomatic young adult. Because the hilum is an unusual location for a bronchogenic cyst, and distinction from a necrotic tumor or lymph node mass cannot be made radiographically, these lesions should be biopsied or removed.

Bilateral Hilar Enlargement

Bilateral hilar enlargement is the result of enlargement of hilar lymph nodes or the central pulmonary arteries (Table 11.9).

Enlarged Lymph Nodes

Malignancy. The malignancies producing bilateral hilar lymph node enlargement are similar to those producing unilateral enlargement. In distinction to unilateral nodal enlargement, metastases are uncommon causes of bilateral hilar nodal enlargement. The most frequent solid tumors producing bilateral hilar disease are small cell carcinoma of the lung, lymphoma, and malignant melanoma.

Bilateral hilar lymph node involvement by lymphoma is more common in Hodgkin disease than NHL. Hilar involvement is virtually never seen without concomitant anterior

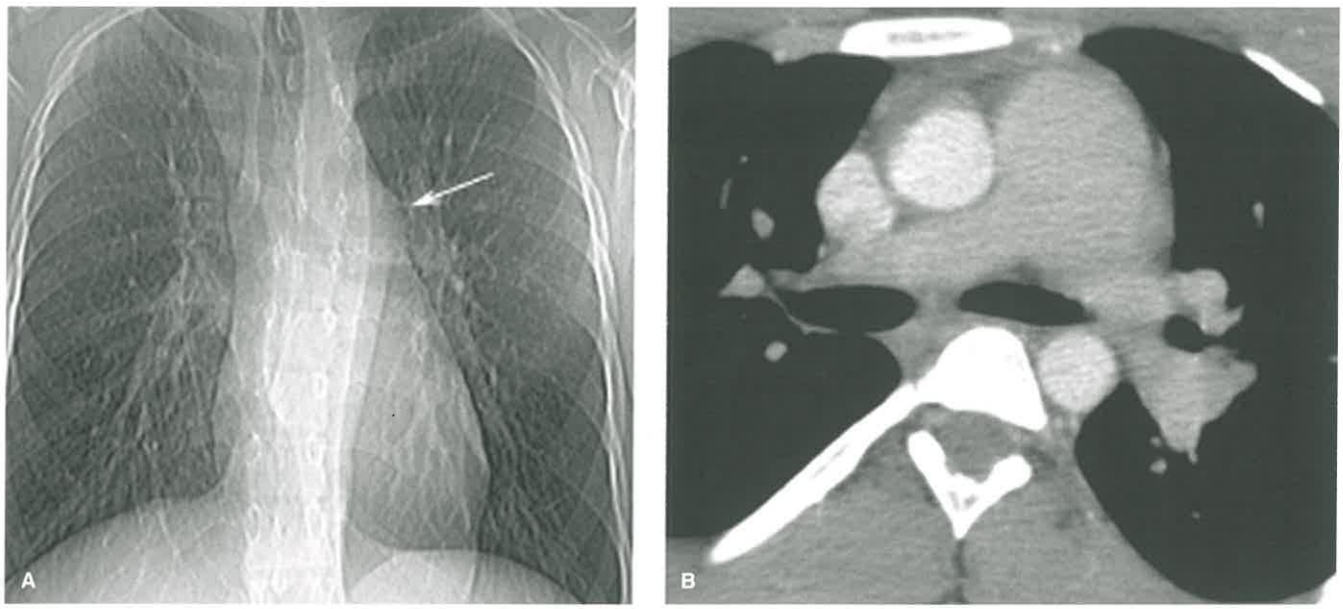

FIGURE 11.34. **Unilateral Hilar Enlargement From Idiopathic Dilatation of the Pulmonary Artery. A:** Scout view from chest CT shows abnormal convexity in the region of the main pulmonary artery (*arrow*). Note thoracic scoliosis. **B:** Enhanced CT scan shows dilated main pulmonary artery with normal right and left pulmonary arteries. Physical examination and echocardiogram showed no evidence of pulmonic valve disease.

mediastinal nodal enlargement in Hodgkin disease, whereas NHL may produce isolated hilar disease.

The most common chest radiographic manifestation of leukemic involvement of the thorax is hilar and mediastinal lymph node enlargement; it is seen in up to 25% of patients. Lymph node enlargement is much more common in the lymphocytic than the myelogenous form, particularly in chronic lymphocytic leukemia.

Infection. Mediastinal and hilar lymph node enlargement from infection is most often seen in tuberculous and fungal infection with histoplasmosis and coccidioidomycosis. In these diseases, the lymph node enlargement may be unilateral or bilateral. With bilateral disease, the enlargement is asymmetric in distinction to sarcoidosis, which is typically symmetric. Bacterial infection from *Bacillus anthracis* (anthrax) and *Yersinia pestis* (plague) may produce bilateral hilar lymph node enlargement. In anthrax infection, the lymph node enlargement is often associated with patchy airspace opacities in the lower lobes. The bubonic form of plague may produce marked hilar and mediastinal adenopathy without pneumonia. Recurrent bacterial infection complicating cystic fibrosis is often associated with bilateral hilar lymph node enlargement, and distinction from pulmonary artery enlargement from pulmonary hypertension may be difficult radiographically.

Sarcoidosis is associated with bilateral hilar lymph node enlargement in 80% of patients. Most of these patients have concomitant paratracheal lymph node enlargement, and nearly half have concomitant radiographic parenchymal disease. The pattern

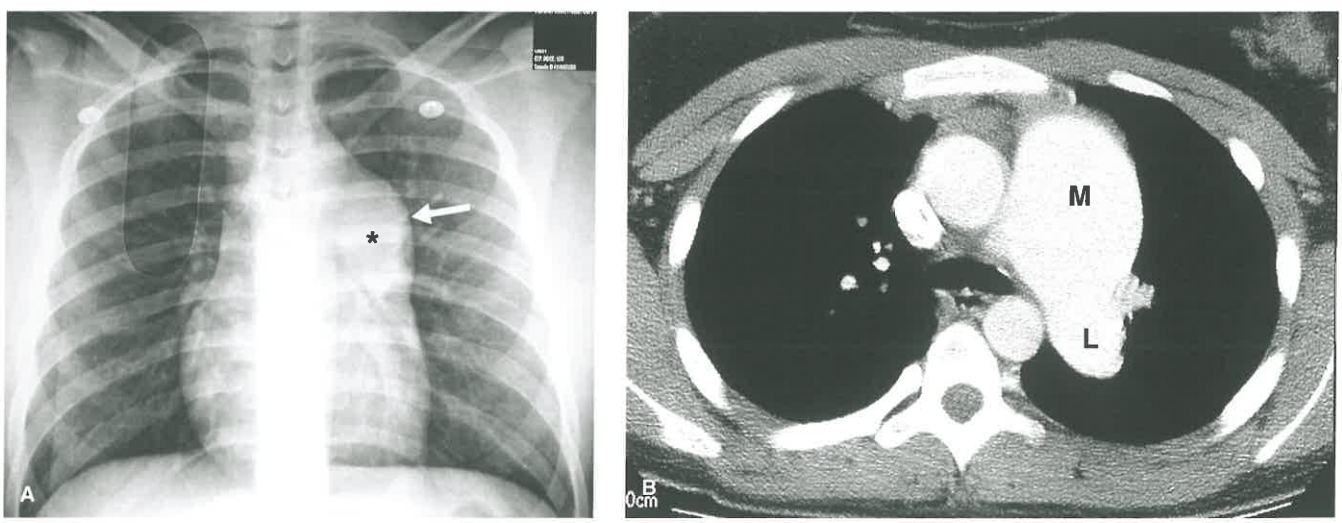

FIGURE 11.35. **Left Hilar Enlargement in Valvular Pulmonic Stenosis. A:** Chest radiograph shows a middle mediastinal mass (*arrow* in [A]) with left hilar enlargement (*asterisk* in [A]). **B:** Axial contrast-enhanced CT shows marked main (M) and left (L) pulmonary arterial dilatation as a result of valvular pulmonic stenosis.

TABLE 11.9

BILATERAL HILAR ENLARGEMENT

Lymph node enlargement	Malignancy	■ Primary intrathoracic malignancy • Non–small cell carcinoma • Small cell carcinoma • Primary pulmonary lymphoma • Carcinoid tumor • Extrathoracic malignancy with nodal spread • Head and neck CA • Breast CA • Genitourinary (renal cell, seminoma) • Melanoma ■ Systemic malignancy • Lymphoma • Leukemia (T cell)
	Infection	■ Tuberculosis ■ Fungal infection • Histoplasmosis ■ Viral infection • Measles • Mononucleosis
	Granulomatous	■ Sarcoidosis ■ Berylliosis
	Inhalational	■ Silicosis
Vascular	Pulmonary artery dilation	■ Pulmonary arterial HTN ■ Increased pulmonary blood flow • Left-to-right shunt • Pulmonary venous HTN • Anemia

of lymph node involvement in sarcoidosis has been termed the 1-2-3 sign, with 1 = right paratracheal, 2 = right hilar, and 3 = left hilar lymph node enlargement (Fig. 11.36). The enlarged nodes produce symmetric, lobulated hilar masses on plain film, since the enlarged nodes remain separate. In 20% of patients, the involved lymph nodes will calcify; usually the calcifications are punctate in appearance, but occasionally peripheral "eggshell" calcification is seen. In some patients, the involved nodes can be seen to enhance after contrast administration on CT. In the majority of patients, the enlarged nodes resolve within 2 years of discovery; in a small percentage, the nodes remain enlarged for many years.

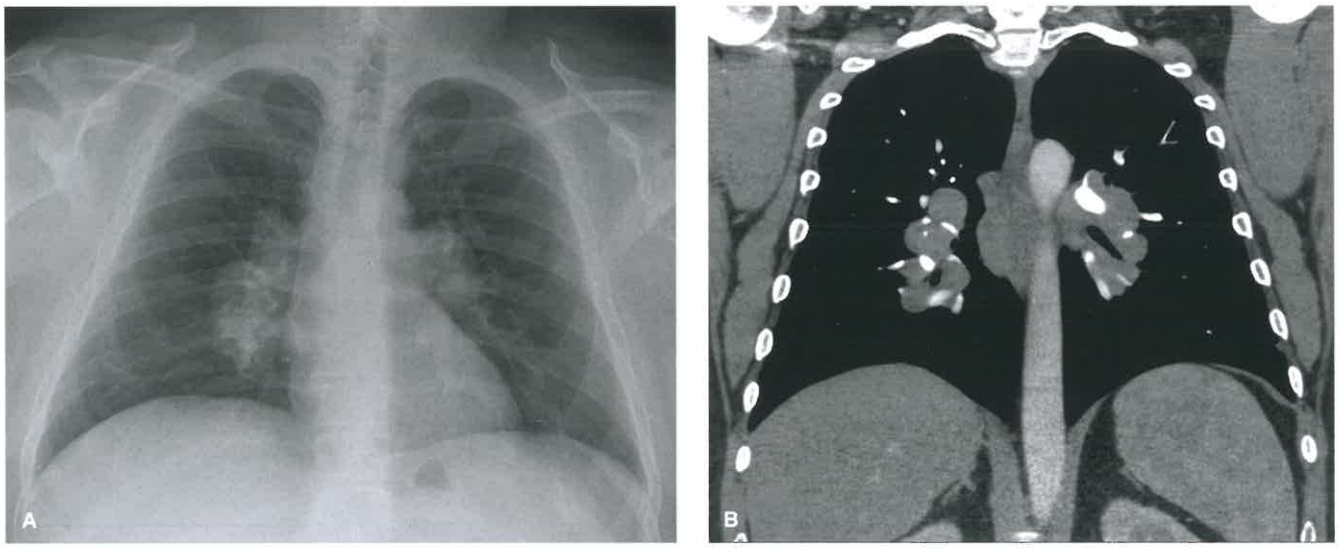

FIGURE 11.36. **Bilateral Hilar Lymph Node Enlargement in Sarcoidosis. A:** Posteroanterior radiograph in a 46-year-old man with sarcoidosis reveals bilateral hilar lymph node enlargement with subtle upper and mid-lung reticulonodular opacities. **B:** Contrast-enhanced coronal CT at the level of the carina shows bilateral hilar lymph node enlargement.

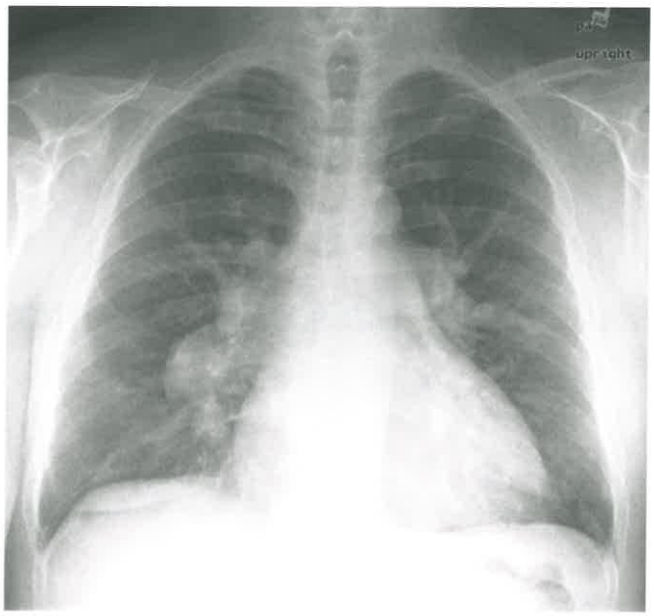

FIGURE 11.37. **Bilateral Hilar Enlargement in Pulmonary Arterial Hypertension.** Frontal chest radiograph shows marked central pulmonary arterial dilatation with attenuation of peripheral vasculature ("pruning") in a patient with severe pulmonary arterial hypertension due to COPD.

Berylliosis and Silicosis. The hilar and mediastinal lymph node enlargement of chronic berylliosis is radiographically indistinguishable from that of sarcoidosis. Similarly, silicosis can produce hilar and mediastinal lymph node enlargement; eggshell calcification of hilar nodes is highly suggestive of this entity, although peripheral nodal calcification may also be seen with sarcoidosis, histoplasmosis, or amyloidosis.

Enlarged Pulmonary Arteries

Bilateral pulmonary artery enlargement is seen with increased flow or increased resistance in the pulmonary circulation (Fig. 11.37). The conditions associated with bilateral pulmonary arterial enlargement are reviewed in Chapter 12.

Small Hila

Bilaterally small hila (Table 11.10) can be seen in some adults with severe pulmonary overinflation from emphysema or in those with diminished pulmonary blood flow due to congenital pulmonary outflow obstruction (tetralogy of Fallot, Ebstein anomaly) or rarely fibrosing mediastinitis.

The most common causes of a small hilum are atelectasis and resection of a portion of lung, which leave a small residual hilar artery supplying the remaining lobe or lobes. Hypoplasia of the pulmonary artery, often with associated abnormalities of the ipsilateral lung (hypogenetic lung syndrome, Swyer–James syndrome) (see Fig. 16.23), is another cause of a small hilum. Less commonly, invasion of the proximal pulmonary artery by mediastinal tumor, or obstruction of the pulmonary artery due to fibrosing mediastinitis, can produce a diminutive hilum. In any patient in whom a small hilum is a new radiographic finding, a CT scan should be performed to assess the mediastinum for central obstructing lesions. The left hilum can appear small in patients in whom the hilar shadow is obscured by the upper left heart margin or by fat in the region of the aortopulmonic interface. In these cases, the lateral radiograph will usually show a left pulmonary artery of normal size.

TABLE 11.10

SMALL HILUM/HILA

Unilateral	Congenital	■ Absence or hypoplasia of the pulmonary artery ■ Pulmonary agenesis, aplasia, hypoplasia ■ Congenital pulmonary venolobar (Scimitar) syndrome (hypogenetic lung)
	Acquired	■ Constrictive bronchiolitis (Swyer–James syndrome) ■ Lobar atelectasis ■ Lobar resection ■ Pulmonary artery narrowing • Fibrosing mediastinitis
Bilateral		■ Emphysema ■ Decreased pulmonary blood flow • Fibrosing mediastinitis • Tetralogy of Fallot • Valvular pulmonic stenosis • Ebstein anomaly

Suggested Readings

Carter BW, Benveniste MF, Madan R, et al. IASLC/ITMIG staging system and lymph node map for thymic epithelial neoplasms. *Radiographics* 2017;37(3):758–776.

Carter BW, Benveniste MF, Madan R, et al. ITMIG classification of mediastinal compartments and multidisciplinary approach to mediastinal masses. *Radiographics* 2017;37(2):413–436.

El-Sherief AH, Lau CT, Wu CC, et al. International association for the study of lung cancer (IASLC) lymph node map: radiologic review with CT illustration. *Radiographics* 2014;34(6):1680–1691.

Inaoka T, Takahashi K, Mineta M, et al. Thymic hyperplasia and thymus gland tumors: differentiation with chemical shift MR imaging. *Radiology* 2007;243(3):869–876.

Katabathina VS, Restrepo CS, Martinez-Jimenez S, Riascos RF. Nonvascular, nontraumatic mediastinal emergencies in adults: a comprehensive review of imaging findings. *Radiographics* 2011;31(4):1141–60.

Kligerman SJ, Auerbach A, Franks TJ, Galvin JR. Castleman disease of the thorax: clinical, radiologic, and pathologic correlation: from the radiologic pathology archives. *Radiographics* 2016;36:1309-1332.

McAdams HP, Kirejczyk WM, Rosado-de-Christenson ML, Matsumoto S. Bronchogenic cyst: imaging features with clinical and histopathologic correlation. *Radiology* 2000;217(2):441–446.

McLoud TC, Kalisher L, Stark P, Greene R. Intrathoracic lymph node metastases from extrathoracic neoplasm. *AJR Am J Roentgenol* 1978;131(3):403-407.

McNeeley MF, Chung JH, Bhalla S, Godwin JD. Imaging of granulomatous fibrosing mediastinitis. *AJR Am J Roentgenol* 2012;199(2):319–327.

Webb WR. Chapter 3. The pulmonary hila. In: Webb WR, Higgins CB, eds. *Thoracic Imaging. Pulmonary and Cardiovascular Radiology*. Philadelphia, PA: Wolters Kluwer; 2017:78–105.

Webb WR. Chapter 6: Lymphoma and lymphoproliferative disease. In: Webb WR, Higgins CB, eds. *Thoracic Imaging. Pulmonary and Cardiovascular Radiology*. Philadelphia, PA: Wolters Kluwer; 2017:179–201.

Whitten CR, Khan S, Munneke GJ, Grubnic S. A diagnostic approach to mediastinal abnormalities. *Radiographics* 2007;27(3):657–671.